Demonstration of Direct-on-filter FTIR to Estimate Silica, Kaolinite, and Calcite Mineral Fraction in Respirable Coal Mine Dust Samples

Nishan Pokhrel

Thesis submitted to the faculty of the Virginia Polytechnic Institute and State University in partial fulfillment of the requirements for the degree of

Master of Science
In
Environmental Engineering

Emily A. Sarver, Chair
Çiğdem Keleş
Linsey Marr

August 13, 2021
Blacksburg, VA

Keywords: FTIR, RCS, silica, kaolinite, calcite, Coal Mine Dust, occupational health

Demonstration of Direct-on-filter FTIR to Estimate Silica, Kaolinite, and Calcite Mineral Fraction in Respirable Coal Mine Dust Samples

Nishan Pokhrel

TECHNICAL ABSTRACT

Respirable coal mine dust (RCMD) has long been recognized as an occupational health hazard. In addition to coal, RCMD can contain minerals such as crystalline silica (i.e., most often present as quartz). There has been a resurgence of lung diseases among US coal miners since the late-1990s which has emphasized the need for better quartz monitoring, and better dust characterization in general. Quartz monitoring in coal mines has traditionally used infrared (IR) spectroscopy-based analytical methods such as the MSHA Method P7 that require significant sample preparation and must be performed in a centralized lab. There are generally thus days to weeks between dust sample collection and reporting of results, which can prevent the prompt mitigation efforts to better control dust and reduce exposures. Recently, a rapid analysis method for quartz has been developed by the US National Institute for Occupational Safety and Health (NIOSH) using direct-on-filter (DOF) Fourier Transform Infrared (FTIR) spectroscopy. The method has been demonstrated in a number of NIOSH-led studies using both laboratory and field samples, and the results show very good accuracy relative to the Method P7 reference. However, it has heretofore not been widely used by others or compared to results from other non-IR analytical methods. Moreover, while FTIR can allow the measurement of additional analytes, this has not yet been a focus of DOF FTIR for RCMD analysis. Analytes such as kaolinite and calcite could be of particular interest in the context of RCMD source apportionment.

In this thesis, the DOF FTIR method is used to estimate silica, kaolinite, and calcite mineral fraction in RCMD samples collected in 16 coal mines, and in the laboratory using dust source materials from those same mines. The results are compared to results from other dust characterization methods such as mass-based thermogravimetric analysis (TGA) and particle-based scanning electron microscopy with energy dispersive X-ray (SEM-EDX). Results indicate the usefulness of the DOF FTIR method, and comparison suggests the presence of significant non-carbonate minerals other than silica and kaolinite in the coal mine dust. The results also show that SEM-EDX frequently indicates more mineral content (primarily other aluminosilicates), than that is predicted by either FTIR or the TGA. Additionally, by focusing mainly on calcite (generally sourced from limestone-based rock dust used in coal mines to prevent coal dust explosion), the second part of this study explores basic source apportionment by analyzing mine samples and samples of major dust source materials (such as run-of-mine coal, rock strata, and rock dust products). Results show that calcite can serve as a suitable proxy for rock dust in coal mine dust, and the results are consistent with expectations surrounding the contribution of dust from different mine locations and sample sources. Additionally, the DOF FTIR also showed good agreement with the TGA and SEM-EDX.

Demonstration of Direct-on-filter FTIR to Estimate Silica, Kaolinite, and Calcite Mineral Fraction in Respirable Coal Mine Dust Particles

Nishan Pokhrel

GENERAL AUDIENCE ABSTRACT

Respirable dust generated in coal mines has long been recognized as an occupational health hazard. In addition to coal, coal mine dust can contain minerals such as crystalline silica, which is particularly hazardous. Since the mid-1990s, there has been an alarming and unexpected increase in lung diseases in coal miners. Respirable crystalline silica is assumed to be a likely causal factor for this resurgence of lung diseases, and this has emphasized the need for better respirable crystalline silica monitoring and to better understand coal mine dust composition. The standard method of measurement of silica (called the MSHA Method P7) generally takes days to weeks between dust sample collection and reporting of results, which can prevent the mine from taking prompt mitigative efforts to better control dust and reduce exposures. Recently, a rapid analysis method for silica has been developed by the US National Institute for Occupational Safety and Health (NIOSH) called the DOF FTIR (direct-on-filter Fourier Transform Infrared Spectroscopy). This method has been shown to have very good accuracy relative to the standard method (MSHA P7). However, it has heretofore not been widely used by others or compared to results from other analytical methods. Moreover, DOF FTIR can also be used to estimate other minerals of interest such as kaolinite and calcite, which can be important in the context of understanding coal mine dust sources.

In this thesis, the DOF FTIR method is used to estimate silica, kaolinite, and calcite mineral fraction in coal mine dust samples collected in 16 coal mines, and in the laboratory using dust source materials from those same mines. The results are compared to results from other dust analysis methods such as mass-based TGA (thermogravimetric analysis) and particle-based SEM-EDX (scanning electron microscopy with energy dispersive X-ray). Results indicate the usefulness of the DOF FTIR method, and comparison suggests the presence of significant non-carbonate minerals other than silica and kaolinite in the coal mine dust. The results also show that SEM-EDX frequently indicates more mineral content than that is predicted by either FTIR or the TGA. Additionally, by focusing mainly on calcite—which is generally sourced from limestone-based rock dust used in coal mines to prevent coal dust explosion—the second part of this study explores the sources of the dust by analysing samples collected in mines, and samples generated in lab from major dust source materials (such as the raw coal, rock strata, and rock dust products obtained from the mines). Results show that calcite can be representative of rock dust in coal mine dust, and the results are consistent with expectations surrounding the contribution of dust from different mine locations and sample sources. Additionally, the DOF FTIR also showed good agreement with the TGA and SEM-EDX.

Acknowledgments

First of all, I would like to show deep gratitude towards my supervisor, Dr. Emily Sarver, first for simply being a wonderful human being, a great mentor, and a great teacher; showing lots of care and support during all my time here, and being so supportive and understanding especially during this time of crisis. I and my family are and always will be very grateful to her for her support.

I would also like to thank my committee members: Dr. Çiğdem Keleş for her prompt support and guidance, and her expertise with the SEM-EDX and data analysis; and Dr. Linsey Marr for encouraging me to get involved in this research.

I would also like to thank the US National Institute of Occupational Safety and Health (NIOSH) and Alpha Foundation for the Improvement of Mine Safety and Health for supporting and sponsoring the projects.

I would also like to extend a special thanks to my research colleague Lizeth Jaramillo for being a great friend, for being very supportive and helpful, and I am grateful for her extensive efforts with the TGA analysis and sample collection.

I would like to thank my dad for always being there, and my mom: without her unwavering support I would not have dreamt of pursuing my studies in this wonderful university; my wonderful sister for all the wonderful conversations, arguments, and fights over the years.

Finally, I would like to thank my significant other for being my anchor, for all the love, dedication and work she has put in me, for helping me go through tough times and decisions; and without her, I seriously would not be where I am today. She deserves all the happiness in the world, and I'm grateful to be a part of her life.

Attribution

Several people aided in the writing and research behind the chapters presented as part of this thesis. A brief description of the contribution of the co-authors (based on CRediT taxonomy) to chapter 1 (titled 'Comparison of mineral content in respirable coal mine dust samples estimated using FTIR, TGA, and SEM-EDX.'), and chapter 2 (titled 'Direct-on-filter FTIR Spectroscopy to estimate calcite as a proxy for limestone 'rock dust' in respirable coal mine dust samples') are provided in the table below.

CRediT Taxonomy	Contributions to	
	Chapter 1	**Chapter 2**
Conceptualization	E. Sarver, N. Pokhrel	E. Sarver, N. Pokhrel
Methodology	E. Sarver, N. Pokhrel	E. Sarver, N. Pokhrel
Validation	N. Pokhrel	N. Pokhrel
Formal Analysis	N. Pokhrel, C. Keles, E. Agioutanti	N. Pokhrel, C. Keles, L. Jaramillo, E. Agioutanti
Investigation	N. Pokhrel, C. Keles, E. Agioutanti	N. Pokhrel, C. Keles, L. Jaramillo, E. Agioutanti
Resources	E. Sarver	E. Sarver
Writing—original draft preparation	N. Pokhrel	N. Pokhrel
Writing—review and editing	E. Sarver	E. Sarver
Visualization	N. Pokhrel	N. Pokhrel
Supervision	E. Sarver	E. Sarver
Project Administration	E. Sarver, C. Keles	E. Sarver, C. Keles
Funding Acquisition	E. Sarver	E. Sarver

Table of Contents

List of Figures

List of Tables

Preface

Chronic exposure to respirable coal mine dust (RCMD) is known to be an occupational health hazard and causes the development of lung diseases such as coal workers' pneumoconiosis (CWP, also known as Black Lung) and silicosis. Especially, respirable crystalline silica (RCS) contained in the coal dust is considered to be particularly hazardous. There has been a recent resurgence of occupational lung disease among US coal miners, with geographic clustering in central Appalachia where miners have been affected more by the most severe and rapidly progressive forms of the disease (e.g., progressive massive fibrosis, PMF).

Radiographic and pathologic studies have indicated that RCS exposure is one of the primary causal factors driving this disease resurgence. This has renewed efforts to improve RCS monitoring in coal mines. RCS in coal mines is typically measured using the standard MSHA Method P7, which uses infrared spectroscopy to estimate the mass of silica in a dust sample. (It is noted here that quartz is well established as the primary form of crystalline silica in coal mine environments, and the terms quartz and silica are therefore often used interchangeably). The sample preparation and equipment requirements of the Method P7 means that it is limited to centralized labs. This can cause a lag time of days to weeks between sample collection and reporting of results, thus preventing the mines to quickly mitigate hazardous exposure conditions.

To enable rapid quartz measurement in RCMD samples, the US National Institute for Occupational Safety and Health (NIOSH) has been working on developing a direct-on-filter (DOF) method using a portable Fourier Transform Infrared Spectroscopy (FTIR) instrument. Even though this method does not provide real-time measurement, it is considerably faster than the standard method and analysis can be done directly without any sample preparation at the end of a worker's shift. While not a focus to date, this method is also suitable for mine engineering studies and research purposes. Further, since an infrared spectrum of the dust on the sample filter is obtained, the DOF FTIR method might be used to estimate RCMD constituents other than silica—including minerals such as kaolinite and calcite.

Ongoing work in the author's research group has focused on other dust characterization methods such as thermogravimetric analysis (TGA) and scanning electron microscopy with energy dispersive X-ray (SEM-EDX). When used on the same (or replicate) samples, these methods can serve as validation for the DOF FTIR. TGA is a mass-based method that can provide estimates of coal, carbonates, and non-carbonate mineral fractions of RCMD. SEM-EDX, on the other hand, is a particle-based method that can be used to size and classify individual particles into predefined mineralogy classes. Table P-1 shows the comparable minerals across each of the three methods.

Table P-1. Comparable constituents across each of the three methods: FTIR, TGA, and SEM-EDX. Description of the constituents is provided in Chapter 1. Description of the constituents are as follows: Q – silica; K – kaolinite; S – silica; ASK – kaolinite; ASO – other aluminosilicates; SLO – other silicates; M – heavy minerals; CB – carbonates; C – carbonaceous; MC – mixed carbonaceous.

	Comparison of constituents attributed to likely sources				
Method	**rock strata**			**rock dust products**	**coal**
FTIR	Silica (Q)	Kaolinite (K)	*Q + K*	Calcite	-
TGA	-	-	non-carbonate minerals	carbonates	coal
SEM-EDX	S	ASK	S + ASK + ASO + SLO + M	CB	C + MC

In this thesis, Chapter 1 compares the quartz and kaolinite mass fractions estimated using the DOF FTIR method, with comparable mineral fractions from TGA and SEM-EDX. This chapter was peer-reviewed and published in the proceedings of the 18th North American Mine Ventilation Symposium, 2021. (The paper is being "Reproduced with permission of The Licensor through PLSclear.")

In Chapter 2, the DOF FTIR method is demonstrated for estimating calcite as a proxy for limestone 'rock dust' in RCMD samples, which is of interest for RCMD source apportionment. Chapter 2 has been published on August, 2021 in the *Minerals* journal (in the special issue 'Mineralogy and Characteristics of Occupational and Environmental Dust Exposures').

Chapter 3 encapsulates all of the available FTIR calibration curves and equations to estimate silica, kaolinite, and calcite mineral fraction in different sampling conditions/setups, along with LOD/LOQ values for the FTIR instrument.

Chapter 4 includes the overall conclusions of the research presented in this thesis and recommendations for future work.

Chapter 1 – Comparison of mineral content in respirable coal mine dust samples estimated using FTIR, TGA, and SEM-EDX

Nishan Pokhrel, Eleftheria Agioutanti, Cigdem Keles, Setareh Afrouz, and Emily Sarver

Citation: Pokhrel, N., et al. (2021). Comparison of mineral content in respirable coal mine dust samples estimated using FTIR, TGA, and SEM-EDX. 18th North American Mine Ventilation Symposium.

ABSTRACT

Since the mid-1990s, there has been a resurgence of severe lung disease among US coal miners. This has prompted efforts to better characterize and monitor respirable dust exposures—especially with respect to mineral content sourced from rock strata surrounding the coal, which is believed to play a central role in many cases of disease. Recently, a rapid analysis method for silica (quartz) has been developed using direct-on-filter Fourier-transform infrared (FTIR) spectroscopy. It can also be used to determine kaolinite, presumably a primary silicate mineral in many coal mines. Other methods, including thermogravimetric analysis (TGA) and scanning electron microscopy with energy dispersive x-ray (SEM-EDX), can also be used to estimate mineral content in respirable coal mine dust. However, there have been few efforts to compare results across multiple methods. This study compares estimates of mineral content derived from FTIR, TGA, and SEM-EDX on respirable dust samples collected in 16 underground coal mines across the US.

1. INTRODUCTION

Exposure to respirable dust has long been recognized as an occupational health hazard to coal mine workers (IARC, 1997; NASEM, 2018). Respirable crystalline silica (RCS) contained in the dust can be particularly hazardous (Castranova & Vallyathan, 2000; Laney & Weissman, 2014; Schatzel, 2009). Indeed, RCS has been cited as a likely causal factor in a dramatic resurgence of severe and rapid lung diseases among coal miners in central Appalachia over the past two decades (Almberg et al., 2018; Blackley et al., 2016; CDC, 2006). This has renewed efforts to improve RCS monitoring in coal mines (Ashley et al., 2020; Cauda et al., 2016; Miller et al., 2013). Moreover, based on knowledge gaps surrounding the whole composition of respirable coal mine dust, and its variability with different geologic and mining conditions, there have been calls to better characterize the dust in general (NASEM, 2018).

Traditionally, measurement of silica in US coal mines is done using the MSHA P7 Standard Method (MSHA, 2008). It uses infrared spectroscopy (IR) to analyze the quartz mass in a dust sample, following ashing of the sample filter. (It is noted that quartz is well established as the primary form of crystalline silica in coal mine environments, and the terms quartz and silica are often used interchangeably.) However, because of the sample preparation and equipment required for the P7 analysis, it is practically limited to centralized labs. This translates to considerable lag time (days to weeks) between sample collection and reporting of results—which impedes swift mitigation of hazardous exposure conditions (Cauda et al., 2016; Miller et al., 2012).

To address this issue, the US National Institute for Occupational Safety and Health (NIOSH) has been working to develop a new direct-on-filter (DOF) approach for quartz measurement (Cauda et al., 2016; Miller et al., 2013; Miller et al., 2012; Miller et al., 2017). Like

Method P7, this method analyzes the quartz in a filter sample. While it is not a real-time measurement, it requires no sample preparation and uses a portable Fourier-transform infrared (FTIR) instrument, such that the analysis can be done immediately after sample collection. Miller et al. found strong linear correlations (ranging from 0.90 – 0.97) between DOF and P7-derived quartz data, demonstrating its potential as an end-of-shift method (Miller et al., 2012).

Although the primary focus of the DOF-FTIR method has been on quartz measurement, it has the potential to provide broader insights to the range of mineral constituents that make up respirable coal mine dust (Cauda et al., 2016; Miller et al., 2017). Similar to determination of quartz from its characteristic peaks in the FTIR spectrum, other minerals can also be identified and possibly quantified from the spectrum. In fact, kaolinite, which is generally expected to be one of the predominant silicate minerals in many coal mine environments (Schatzel, 2009; Su et al., 2020), is already an integral part of the quartz quantification method; kaolinite has an overlapping peak with quartz, and this interference is quantified (in terms of spectrum peak area) in order to analytically correct the quartz measurement (Cauda et al., 2016; Lee et al., 2013; Miller et al., 2012). Thus, kaolinite mass (K), along with quartz (Q), can be easily reported from the DOF-FTIR analysis of coal mine dust samples using calibration curves for each analyte. It is possible that other minerals of interest can be reported too (e.g., calcite, which could serve as crude surrogate for respirable dust sourced from limestone rock dusting products being used in a mine).

In addition to FTIR, other analytical methods can also be used to characterize respirable coal mine dust. Thermogravimetric analysis (TGA) is a mass-based method that the authors' research group recently applied to determine coal, non-carbonate minerals, and carbonates fractions of dust, which can be loosely associated with dust sources related to coal cutting, rock strata cutting/drilling, and rock dust application, respectively, in many mines (Agioutanti et al., 2020). TGA basically tracks the weight change of a sample with temperature in a controlled environment. Since coal, carbonates, and non-carbonates have their own thermal behavior (i.e., coal and carbonates tend to lose mass in characteristic temperature regions, while the non-carbonate minerals of interest like silica and silicates tend to be inert in those regions), the sample behavior can be used to estimate these three primary fractions (Agioutanti et al., 2020). Further, if rock-strata sourced dust in a coal mine is dominated by silica and silicates, the non-carbonate minerals fraction might be comparable to the Q+K per the FTIR (Table 1-1).

Scanning electron microscopy with energy dispersive X-ray (SEM-EDX) analysis is a particle-based method that can be used to size and classify individual particles. For respirable coal mine dust, the authors' group has established routines to bin particles into the following predefined mineralogy classes: carbonaceous (C) and mixed carbonaceous (MC), which are generally associated with coal dust and/or diesel particulates (in the very fine sizes); alumino-silicates (AS, which can be further sub-classified as either kaolinite ASK, or other alumino-silicates, ASO), other silicates (SLO), silica (S), and metal oxides and sulfides (M), which are generally associated with rock-strata sourced dust; carbonates (CB), which are associated with rock dust (e.g., limestone) application in most US mines; and others (O), which are particles not otherwise classified (Johann-Essex, Keles, & Sarver, 2017; Sarver et al., 2019). It stands to reason that distribution of dust across these classes might also be comparable to FTIR and TGA measures per Table 1-1/

Table 1-1. Comparable constituents across each of the three methods.

	Comparison of constituents attributed to likely sources				
Method	**rock strata**			**rock dust products**	**coal**
FTIR	Q	K	Q + K	-	-

TGA	-	-	non-carbonate minerals	carbonates	coal
SEM-EDX	S	ASK	S + ASK + ASO + SLO + M	CB	C + MC

Though FTIR, TGA, and SEM-EDX can all be used to measure certain constituents of respirable coal mine dust, they have not been directly compared. The primary goal of the current study is to compare mineral content, specifically, estimated using all three methods. For this, samples from different locations in 16 underground US coal mines were analyzed. Notably, the study also represents an early application of the DOF-FTIR method for dust characterization research.

2. MATERIALS AND METHODS

2.1 Sample Collection

Respirable dust samples were collected in 2018 from 16 different US underground coal mines (numbered 10-25), representing five mine regions: northern Appalachia (NA, mines 7-9), central Appalachia (CA, mines 10-15, 21, 22, 25), western coal basin (W, mines 23 and 24), and mid-western Illinois coal basin (MW, mines 19 and 20). A total of 93 sets of samples (each containing multiple replicates) were collected in several key locations in each mine: near the coal 'feeder (F)' or along the main conveyor belt; near the 'intake (I)' (including near the headgate of a longwall); near major 'production (P)' activities (i.e. downwind of a continuous miner or along the longwall face); in the 'bolter (B)' (i.e. just downwind of an active roof-bolter); and in the 'return (R)' (including near the tailgate of a longwall). Each sample set was collected over about 2-4 hours.

Escort ELF air sampling pumps with a 10-mm nylon Dorr-Oliver cyclone at a flow rate of 2.0 lpm (yielding a d50 of about 3.5 μm) were used to collect dust onto 37-mm filters in two-piece styrene cassettes. For the FTIR analysis, the samples were collected onto polyvinyl chloride filters (PVC, 5.0 μm pore size), while for SEM and TGA, polycarbonate filters (PC, 0.4 μm pore size) were used (Agioutanti et al., 2020; Johann-Essex, Keles, Rezaee, et al., 2017; Sarver et al., 2019). The PVC filters were pre- and post-weighed using a microbalance (Sartorius MSE6.6S, Gottingen, Germany) to determine the total dust mass.

2.2 FTIR Analysis

For each sample set, one PVC filter was prepared for analysis by an ALPHA II FTIR Spectrometer (Bruker optics, Billerica, MA) to get the absorbance spectra between spatial frequencies of 4000 cm^{-1} to 400 cm^{-1}. The PVC filters were carefully taken out from the 2-piece cassettes and placed onto FTIR-compatible 4-piece cassettes (Zefon International, Ocala, FL), which were then mounted centrally onto a sample holder within the chamber of the FTIR instrument. Sixteen scans of the center 6-mm diameter spot on each filter were taken at a resolution of 4 cm^{-1} using Blackman-Harris three-term apodization, which then underwent a rubber band baseline correction with 64 baseline points (to remove distortions) (Miller et al., 2012; Miller et al., 2017).

Being a direct-on-filter approach, the FTIR spectra obtained on a dust sample also includes the absorbance data of the filter material. This was addressed by subtracting the background spectrum of a blank PVC filter. Blank filter data was obtained for each batch of dust samples analyzed by FTIR to ensure that any effect of environmental conditions (e.g., humidity) was minimized.

In an absorbance spectrum for a pure sample, quartz appears as a doublet peak at 780 and 800 cm^{-1}, while kaolinite appears as a larger peak at 915 cm^{-1} and a smaller peak at 790 cm^{-1}. Using Bruker's OPUS software (Version 8.2.28, 32 bit), the spectral region between 816-767 cm^{-1} (corresponding to the doublet peak for Q) and between 930-900 cm^{-1} (corresponding to the larger peak for K) was integrated to find the peak areas, using calculations consistent with other IR methods for quartz analysis (Miller et al., 2012; MSHA, 2008). Since the smaller peak of K lies in the same range for quartz doublet peak, the Q peak area was corrected for this interference using a previously calculated correction ratio of 3.8 for the FTIR instrument (Miller et al., 2012; Miller et al., 2017). This was done using the following equation (Miller et al., 2012):

Equation 1-1:
$$Corrected\ Q\ peak\ area = Q\ peak\ area - \frac{K\ peak\ area}{3.8}$$

These peak areas of the 6-mm spot on the filter center were extrapolated to determine the total Q and K masses on the entire 37-mm filter. This was done using previously established calibration curves developed by NIOSH from regression analysis of the peak integrated area versus the gravimetric mass of pure crystalline silica (MIN-U-SIL 5), kaolinite, or a mixture of the two aerosolized in a calm-air laboratory dust chamber (Cauda et al., 2016; Miller et al., 2017; NIOSH, 2019). It is important to note that those calibration curves were developed with samples collected in 3-piece cassettes (again using 10-mm nylon Dorr-Oliver cyclones at 2 LPM flowrate). Since the mine samples used in this study were collected in 2-piece cassettes—which promote a slightly different dust loading pattern—the FTIR-derived Q and K mass results were also corrected using a previously established correction factor of 0.877 (Miller et al., 2013). Finally, the quantified masses were converted to mass percentages using total mass of the samples.

2.3 TGA Analysis

One PC filter from each sample set was used for TGA per Agioutanti et al. (2020). Briefly, dust was recovered from the sample filters by sonication in isopropanol, redeposited in a clean, tared sample pan, and analyzed by a Q500 Thermogravimetric Analyzer (TA Instruments, New Castle, DE) using the prescribed thermal ramping routine. (Notably, the same instrument used by Agioutanti et al. was used here.) Agioutanti et al. showed that weight change in several regions of interest could be used to estimate the coal, carbonates, and non-carbonate minerals mass fractions in the sample; and published a series of mass balance equations that can be applied to a sample thermogram for this purpose. These were applied to all sample thermograms here.

2.4 SEM-EDX Analysis

Finally, one PC filter from each sample set was also analyzed by the SEM-EDX. Dust samples were prepared and analyzed based on a previously established method in Sarver et al. (2019), with a computer-controlled routine using an FEI Quanta 600 FEG environmental scanning electron microscope (ESEM) (Hillsboro, OR, USA) equipped with a backscatter electron detector (BSD) and a Bruker Quantax 400 EDX spectroscope (Ewing, NJ, USA) (Johann-Essex, Keles, Rezaee, et al., 2017; Johann-Essex, Keles, & Sarver, 2017; Sarver et al., 2019). This routine, using Bruker's Esprit software (Version 1.9.4), was used to scan multiple areas across each sample in order to analyze about 800 particles per sample. For each particle, the long and intermediate dimensions were recorded, and its elemental spectra were used to classify its mineralogy (Table 1-2). These data were then used to estimate the particle's mass. The volume was calculated using

the long and intermediate dimensions of the particle and its assumed thickness (or short dimension); assumptions for short-to-intermediate dimension ratio (SI) and specific gravity (SG) are shown in Table 1-2 for each class. Computed particle masses in each class were summed and divided by the total particle mass for the sample to estimate the mass fraction (%) for each class, which were then compared to the FTIR and TGA results.

Table 1-2. SEM-EDX classification criteria for supramicron particles, along with assumptions for S:I ratio and SG for each mineralogy class (updated from Johann-Essex et al., 2017b).

	Atomic %								Particle size to mass assumptions	
Class	**O**	**Al**	**Si**	**C**	**Mg**	**Ca**	**Ti**	**Fe**	**SI**	**SG**
C	<29	≤0.3	≤0.3	≥75	≤0.5	≤0.41	≤0.06	≤0.15	0.6	1.4
MC		≤0.35	<0.35		≤0.5	≤0.5	≤0.6	≤0.6	0.6	1.4
ASK[1]		≥0.35	≥0.35		(<15)	(<8)	(<13)	(<13)	0.4	2.6
ASO[1]		≥0.35	>0.35		(≥15)	(≥8)	(≥13)	(≥13)	0.4	2.6
SLO[2]			≥0.33						0.4	2.6
S[3]			≥0.33						0.7	2.65
M		>1					>1	>1	0.7	4.96
CB	>9				>0.5	>0.5			0.7	2.7

[1]To differentiate ASK from ASO, additional limits for Al, Si, Mg, Ca, Ti and Fe are shown in parenthesis (normalized to exclude C and O)

[2]Additional limits for SLO: Si/(Al+Si+Mg+Ca+Ti+Fe) < 0.5

[3]Additional limits for S: Al/Si < 1/3 and Si/(Al+Si+Mg+Ca+Ti+Fe) ≥ 0.5

3. RESULTS AND DISCUSSION

Table 1-3 summarizes the FTIR, TGA, and SEM-EDX results from all 93 sets of respirable mine dust samples included in the study. It is noted that the TGA recovered mass refers to the sum of the coal, carbonates, and non-carbonate minerals masses determined for each PC sample analyzed. However, this may not match the total sample mass for the paired PVC filter due to several factors including differences in total mass collected on each filter (i.e., due to differences in the filter media themselves or spatial variation in the sampling environment), and less than 100% recovery of dust from the PC filter. That said, PVC sample mass and TGA recovered mass do generally trend together.

Table 1-3. Summary of results for 93 sets of respirable coal mine dust samples.

Samp.	Mine		Samp.	PVC Sample	TGA	FTIR (mass %)		TGA (mass %)			SEM-EDX (mass %)							
No.	**Reg.**	**No.**	**Loc.**	**Mass (mg)**	**Recovered Mass (mg)**	**Q**	**K**	**Coal**	**Carb.**	**Non-carb.**	**C**	**MC**	**ASK**	**ASO**	**S**	**SLO**	**M**	**CB**
1	SCA	10	B	0.148	0.146		24.7	25.4	3.7	70.9	17.8	16.6	25.7	32.7	5.6	0.0	0.8	0.8
2	SCA	10	B	0.181	0.198		26.4	26.8	5.5	67.7	3.8	8.9	47.1	35.3	3.7	0.0	0.3	1.0
3	SCA	10	F	0.132	0.157		23.6	41.7	3.5	54.8	11.3	7.9	32.3	35.3	8.3	0.0	3.9	0.9
4	SCA	10	F	0.183	0.064		18.3	43.6	16.8	39.6	8.3	7.7	37.0	44.2	1.0	0.0	2.0	0.0
5	SCA	10	I	0.005	0.049		n/a*	84.4	1.8	13.7	22.6	14.0	5.4	9.1	41.0	1.3	0.4	6.2
6	SCA	10	P	0.089	n/a		29.9	n/a	n/a	n/a	n/a	n/a	n/a	n/a	n/a	n/a	n/a	n/a
7	SCA	10	P	1.494	1.286		21.3	22.7	3.2	74.1	0.0	0.0	83.5	15.8	0.7	0.0	0.0	0.0
8	SCA	10	R	0.038	0.074		38.1*	62.3	3.3	34.4	28.0	13.2	23.8	24.9	8.3	0.2	0.3	1.3
9	SCA	11	B	0.106	0.042		24.4	36.0	9.3	54.7	1.2	5.2	11.8	60.4	14.2	0.2	1.2	5.8
10	SCA	11	F	0.164	0.104		14.2	54.4	6.9	38.7	23.5	10.8	11.2	30.0	11.1	0.0	7.8	5.6
11	SCA	11	P	1.153	0.666	6.2	11.9	11.4	4.9	83.7	0.0	0.1	3.8	95.4	0.8	0.0	0.0	0.0
12	SCA	11	R	0.749	0.137	6.7	13.9	25.8	5.2	69.0	0.0	0.0	1.8	97.5	0.7	0.0	0.0	0.0
13	SCA	12	B	0.103	0.031		21.0	55.1	13.4	31.4	32.1	16.5	9.7	19.0	4.2	1.0	1.4	16.1
14	SCA	12	I	0.054	0.074		35.3	76.0	5.4	18.6	56.7	8.2	7.0	11.7	5.3	0.0	0.0	11.1
15	SCA	12	P	1.077	0.486	4.0	12.8	29.5	4.8	65.6	7.0	7.5	29.6	52.0	3.4	0.0	0.4	0.0
16	SCA	12	R	0.649	0.430	3.2	15.3	20.8	7.4	71.7	0.1	0.6	7.2	91.3	0.7	0.0	0.0	0.1
17	SCA	13	B	2.535	3.405	12.3	10.1	13.6	5.8	80.6	0.0	0.0	2.1	96.8	1.1	0.0	0.0	0.0

18	SCA	13	F	0.189	0.057		8.4*	78.0	8.1	14.0	36.1	8.4	2.1	7.6	1.1	2.2	1.2	41.2
19	SCA	13	I	0.035	0.030		43.2*	39.9	26.8	33.3	6.5	1.0	1.3	5.7	1.4	0.1	0.0	84.1
20	SCA	13	I	0.701	0.125	4.6	5.9	62.9	12.8	24.4	23.1	10.5	3.7	41.3	7.0	0.0	0.3	14.0
21	SCA	13	R	7.347	11.346	4.7	1.5	8.1	69.5	22.4	0.0	0.0	0.0	9.5	0.0	5.4	0.0	85.0
22	SCA	13	R	1.297	1.312	1.8	2.6	73.9	4.4	21.7	58.9	10.8	5.4	15.4	4.1	0.0	0.1	5.4
23	SCA	14	B	0.039	0.055		42.8*	29.0	12.5	58.6	10.5	6.9	27.9	32.2	16.6	0.0	2.6	3.2
24	SCA	14	F	0.187	0.213		19.1	27.5	5.1	67.4	2.3	4.5	10.6	53.3	13.2	2.1	1.4	12.7
25	SCA	14	I	0.002	0.055		n/a*	66.7	9.2	24.1	8.6	3.8	4.3	16.8	8.7	0.0	0.0	57.9
26	SCA	14	P	4.348	3.682	7.3	11.3	9.5	4.7	85.8	0.0	0.0	2.0	97.9	0.1	0.0	0.0	0.0
27	SCA	21	B	0.085	0.029		20.5*	46.5	10.2	43.3	4.7	8.4	7.9	37.2	15.1	0.1	1.2	25.4
28	SCA	21	F	0.089	0.030		21.0	15.8	2.8	81.5	6.3	10.1	15.9	47.9	11.8	0.0	3.3	4.6
29	SCA	21	I	0.063	0.064		27.6*	60.8	5.6	33.6	7.8	8.7	18.4	42.8	10.1	0.0	2.0	10.1
30	SCA	21	P	1.415	1.757	5.2	12.0	8.1	4.1	87.9	0.0	0.0	1.5	98.1	0.4	0.0	0.0	0.0
31	SCA	21	R	0.557	1.086	4.4	12.8	8.7	4.2	87.1	0.0	0.0	5.4	93.7	0.8	0.0	0.0	0.0
32	SCA	22	F	0.018	0.021		78.1*	61.9	5.2	33.0	40.0	10.6	3.9	9.7	6.3	0.0	26.5	3.0
33	SCA	22	I	0.003	0.003		n/a*	89.7	6.3	4.1	40.3	11.6	9.5	19.3	8.8	0.0	1.3	9.2
34	SCA	22	P	1.230	0.339	7.0	7.2	34.2	16.3	49.5	0.0	0.0	0.5	98.2	1.3	0.0	0.0	0.0
35	SCA	25	B	0.416	0.286	8.65	21.7	39.0	6.1	54.9	0.0	0.3	18.0	76.7	5.0	0.0	0.0	0.0
36	SCA	25	F	0.336	0.460	5.63	13.0	40.3	8.3	51.8	2.7	7.5	9.6	64.2	6.7	0.2	2.5	6.6
37	SCA	25	I	0.010	0.026			77.4	0.7	21.8	7.2	9.1	17.3	43.0	8.6	1.1	1.2	12.5
38	SCA	25	P	0.357	0.191	4.24	19.2	57.3	6.1	36.6	0.5	3.9	15.7	71.0	5.3	0.0	0.7	3.0
39	SCA	25	P	0.189	0.186	4.65	20.8	18.4	7.2	74.4	6.9	11.1	32.6	31.5	12.2	0.0	5.5	0.1
40	SCA	25	P	0.669	0.354	5.59	19.6	42.3	1.0	56.7	0.0	0.7	37.4	59.5	2.1	0.1	0.2	0.0
41	SCA	25	P	0.311	0.064	5.48	21.8	26.9	9.8	63.3	1.9	7.5	23.4	50.0	4.8	0.0	0.8	11.7
42	SCA	25	P	0.227	0.060	3.10	19.8	29.1	1.1	69.8	2.9	6.3	35.9	42.3	7.7	0.1	2.4	2.3
43	SCA	25	P	0.088	0.046	2.62	22.3	42.7	8.3	49.0	6.3	8.8	33.7	28.3	9.1	0.0	2.2	11.7
44	SCA	25	P	0.949	0.330	7.29	19.1	13.9	7.6	78.5	0.0	0.1	28.6	69.7	1.6	0.0	0.0	0.0
45	SCA	25	P	0.596	0.255	7.00	20.2	13.8	5.1	81.1	0.1	0.1	26.5	71.1	0.7	0.0	0.0	1.5
46	SCA	25	R	0.130	0.110	2.41	15.3	22.1	6.2	71.6	11.5	12.6	24.1	24.9	13.7	0.0	0.8	12.4
47	SCA	25	R	0.132	0.021	4.43	24.3	23.3	6.1	70.6	7.3	8.6	27.9	42.4	6.6	0.0	3.8	3.5
48	SCA	25	R	0.069	0.014	8.14	24.9	52.6	20.0	27.4	8.3	9.6	29.5	34.8	6.9	0.1	3.0	7.9
49	SCA	25	R	0.202	0.218	3.03	19.9	18.3	6.3	75.4	11.3	9.1	27.3	32.2	12.0	0.2	5.4	2.5
50	MCA	15	B	0.145	0.065		19.6	30.3	10.8	58.9	14.9	8.4	11.4	24.2	22.7	0.0	5.5	12.9
51	MCA	15	F	0.028	0.008		56.4*	47.8	23.5	28.8	46.3	3.2	15.0	9.6	4.8	0.0	0.0	21.2
52	MCA	15	I	0.001	0.029		n/a*	73.8	-0.1	26.3	8.7	1.4	0.0	6.6	0.0	0.0	0.5	82.7
53	MCA	15	P	0.470	0.085	4.1	23.5	32.1	7.7	60.2	9.6	6.2	27.6	21.4	11.8	0.0	0.0	23.4
54	MCA	15	R	0.351	0.662	5.1	19.6	19.7	6.2	74.0	8.0	5.4	30.5	40.3	11.7	0.0	1.6	2.5
55	NA	16	B	0.089	0.150		21.1	72.1	5.4	22.5	51.0	7.4	10.4	4.7	4.6	0.0	5.2	16.7
56	NA	16	F	0.073	0.067		35.6	65.0	9.0	26.1	41.8	11.2	25.6	10.8	2.5	0.0	0.6	7.7
57	NA	16	P	0.221	0.267		13.3	68.0	7.1	24.9	27.4	22.4	9.9	14.4	9.4	1.6	7.7	7.1
58	NA	16	R	0.172	0.253		14.9	62.3	9.7	28.0	53.5	14.0	7.0	9.5	4.4	0.0	3.7	8.0
59	NA	17	B	0.043	0.023		39.3*	46.3	38.1	15.7	7.2	3.0	3.2	16.4	18.0	1.5	5.6	45.0
60	NA	17	I	0.016	0.220		90.5*	93.2	4.1	2.7	2.4	1.4	1.4	3.4	1.8	0.0	1.5	88.1
61	NA	17	I	0.072	0.151		36.5	61.6	6.3	32.1	24.7	5.3	32.9	19.8	4.0	0.0	0.3	13.0
62	NA	17	P	0.277	0.360		25.6	34.9	4.8	60.3	2.5	5.3	42.2	47.1	0.9	0.0	0.4	1.6
63	NA	17	R	0.763	0.826	1.9	21.5	35.4	3.4	61.3	0.0	0.0	59.0	40.3	0.7	0.0	0.0	0.0
64	NA	17	R	0.489	0.713		5.9	30.7	59.0	10.2	14.8	2.4	1.5	6.8	1.0	0.1	0.9	72.5
65	NA	18	B	0.096	0.087		33.3	31.7	9.8	58.5	26.4	5.7	27.2	20.1	8.3	0.1	4.2	7.9
66	NA	18	F	0.018	0.025		n/a	71.3	6.4	22.3	24.1	5.4	16.2	17.4	4.3	0.5	1.4	30.7
67	NA	18	I	0.002	0.018		n/a*	67.7	12.2	20.1	7.9	1.8	4.0	3.8	1.2	0.0	1.1	80.0
68	NA	18	P	0.340	0.095		21.9	39.5	5.7	54.9	1.0	1.4	38.2	54.5	2.8	0.0	0.0	2.1
69	NA	18	R	0.231	0.113		22.9	41.5	7.7	50.8	21.7	10.5	34.5	25.3	6.8	0.1	0.0	1.1
70	MW	19	B	0.181	0.071		15.1	56.9	9.0	34.1	8.0	21.3	1.4	48.7	7.7	0.0	0.7	12.2
71	MW	19	F	2.608	0.901	4.6	7.7	48.4	6.1	45.5	0.4	1.6	3.8	82.2	10.6	0.2	0.4	0.8
72	MW	19	I	0.014	0.006		76.0*	0.0	48.8	51.3	15.7	13.9	2.5	24.4	4.8	0.8	1.6	36.3
73	MW	19	P	0.277	0.333		8.3	49.5	16.7	33.8	13.6	11.6	0.0	32.4	3.5	0.2	5.8	32.8
74	MW	19	R	0.299	0.319		7.4	45.2	20.6	34.2	9.8	19.9	0.1	37.8	4.2	0.5	2.8	25.0
75	MW	19	R	0.223	0.291		11.2	47.2	5.0	47.8	13.8	19.6	8.0	48.8	5.1	0.2	1.7	2.9
76	MW	20	B	0.530	0.413		9.4	32.0	21.4	46.6	0.0	1.5	0.1	68.1	1.0	0.0	0.7	28.6
77	MW	20	F	0.143	0.024		13.3	32.1	35.9	32.0	27.3	6.0	1.6	16.6	7.8	0.0	2.4	38.4
78	MW	20	F	0.191	0.130		11.2	36.6	21.2	42.2	19.4	10.7	3.5	28.2	6.0	0.1	0.1	32.1
79	MW	20	I	0.019	0.041		54.9*	57.5	28.3	14.1	16.8	7.5	0.5	2.6	3.8	0.6	3.4	64.7
80	MW	20	P	0.758	0.613	0.5*	9.0	31.4	8.6	60.0	0.0	0.0	0.2	94.8	0.6	0.0	0.0	4.3
81	MW	20	R	0.577	0.317		9.7	32.7	11.1	56.2	7.7	19.6	2.9	45.4	2.8	0.0	1.3	20.2
82	W	23	I	n/a	0.231	n/a	n/a*	67.8	18.0	14.3	65.9	3.9	1.5	1.2	4.2	0.0	5.8	17.5
83	W	23	I	0.097	0.051		10.7*	30.6	58.7	10.6	6.3	1.3	0.0	2.2	0.0	0.0	0.0	90.3
84	W	23	I	0.176	0.164		8.3*	40.8	50.7	8.5	15.3	4.3	0.0	1.3	0.8	0.1	0.5	77.7
85	W	23	P	0.349	0.351		3.9*	5.8	68.0	26.2	1.4	0.9	0.0	0.2	0.1	0.0	0.1	97.3
86	W	23	P	0.268	0.215		4.1*	n/a	n/a	n/a	n/a	n/a	n/a	n/a	n/a	n/a	n/a	n/a
87	W	23	R	0.888	1.061		4.1	29.0	62.1	8.9	1.3	1.8	0.0	0.6	0.1	0.0	0.0	96.2
88	W	24	F	0.068	0.134		22.8*	70.9	9.8	19.3	37.0	7.1	0.2	10.7	5.5	0.2	0.1	39.1
89	W	24	I	1.547	1.492	24.9	6.6	30.7	2.9	66.4	0.6	1.3	0.0	3.0	94.6	0.4	0.0	0.0
90	W	24	I	0.052	0.051		21.1*	68.2	15.9	15.9	27.8	7.8	2.0	10.1	4.7	1.2	0.3	46.1
91	W	24	I	0.063	0.064		24.1*	53.0	20.0	27.0	23.6	2.8	0.0	7.5	4.0	1.7	2.3	58.1
92	W	24	R	0.165	0.195		11.8	43.7	14.0	42.3	14.6	7.8	0.4	19.5	20.4	1.8	0.0	35.5
93	W	24	R	5.361	5.312	3.5	3.2	12.3	70.2	17.6	0.3	0.2	0.0	5.7	0.0	0.9	0.0	93.0

*samples between LOD and LOQ
n/a*: data unavailable (these samples are between LOD and LOQ, and have very low/missing sample mass)
n/a: data unavailable
empty cells: samples below LOD

The sample mass (determined from the PVC filters in each set) was generally highest in the P and R sampling locations (mean values of 0.75 and 1 mg, respectively), while masses in the I, B, and F locations were lower (means of 0.2, 0.3, and 0.3 mg, respectively). It is worth noting that sample masses reported here should not be used as a proxy for mass concentration in the sampling location since the sampling time varied. However, the sample mass does have important ramifications for each analytical method. For SEM-EDX, high-mass samples may exhibit dense loading on the filter, which can challenge analysis of individual particles. Though no mass limit has been established, care was taken to avoid analysis on filter areas that may have had overlapping particles. Even so, it is possible that elemental spectra on some particles were influenced by surrounding particles.

For TGA, Agioutanti et al. (2020) found that limits of detection (LOD) and quantification (LOQ) in lab-generated respirable dust samples were on the order of 50 and 150 µg, respectively, of recovered dust for each primary sample component (i.e., coal, carbonate, or non-carbonates). In real mine dust samples, it is impossible to know the component masses *a priori*—rather only the total recovered dust mass is known. Given that the current study represents the first time this TGA method has been used for mine dust samples, LOD and LOQ were not applied strictly here. However, results for particularly low-mass samples should be considered with some caution. (E.g., Using a threshold of 200 µg total recovered dust, about 40 samples per Table 1-3 would be considered low-mass).

Similarly, FTIR results can also be affected by sample mass, and only the total dust mass (on PVC filter) is known *a priori*. Per Cauda et al. (2016), the LOD and LOQ for Q are 5 and 16 µg, respectively; and using the same approach to compute LOD and LOQ, the values for K was estimated as ~5 and ~18 µg, respectively. As shown in Table 1-3, only 27 of the 93 samples had quantifiable Q, with 5 samples between LOD and LOQ, and the rest of them were below LOD (and had total sample mass <350µg). In contrast, 64 of the samples had quantifiable K, and the rest were between LOD and LOQ, with the exception of one sample below LOD.

In summary, higher constituent masses are needed to surpass LOD/LOQ for TGA and FTIR, and thus higher total sample mass is favorable here. On the other hand, lower sample mass is more favorable for SEM-EDX. The relative agreement between results from each method as a function of sample mass can shed more light on these issues and design of sampling campaigns.

3.1 Comparison of the mass-based FTIR and TGA

Comparison of FTIR Q+K with TGA estimation of non-carbonates is shown in Figure 1-1 (a). As expected, these measures tend to increase together, though their ratio varies widely across the entire dataset (Figure 1-1 (a)). For about 60% of the samples pairs, the TGA result is higher than the FTIR result (by a factor of 2-7x), whereas for another 15% of the pairs the FTIR result is higher than the TGA (by up to 4x). Figure 1-1 (b) helps to illustrate the effect of sample mass here.

Based on higher-mass samples, for which both methods are expected to increase in accuracy, the tendency of the TGA result to be significantly higher than the FTIR result indeed suggests that quartz and kaolinite do not account for all of the non-carbonate mineral content in many of these respirable dust samples. Rather, based on the SEM-EDX results (Table 1-3), there appear to be other non-kaolinite alumino-silicates (e.g., feldspars or micas). Specifically, samples with high TGA overestimation of non-carbonates (compared to FTIR) have relatively very high SEM-EDX estimates of ASO. Further analysis of both the SEM-EDX elemental data and the FTIR spectra—in terms of potential peaks related to other silicates/minerals along with potential interferences—could provide useful insights on this topic and will be the focus of future work.

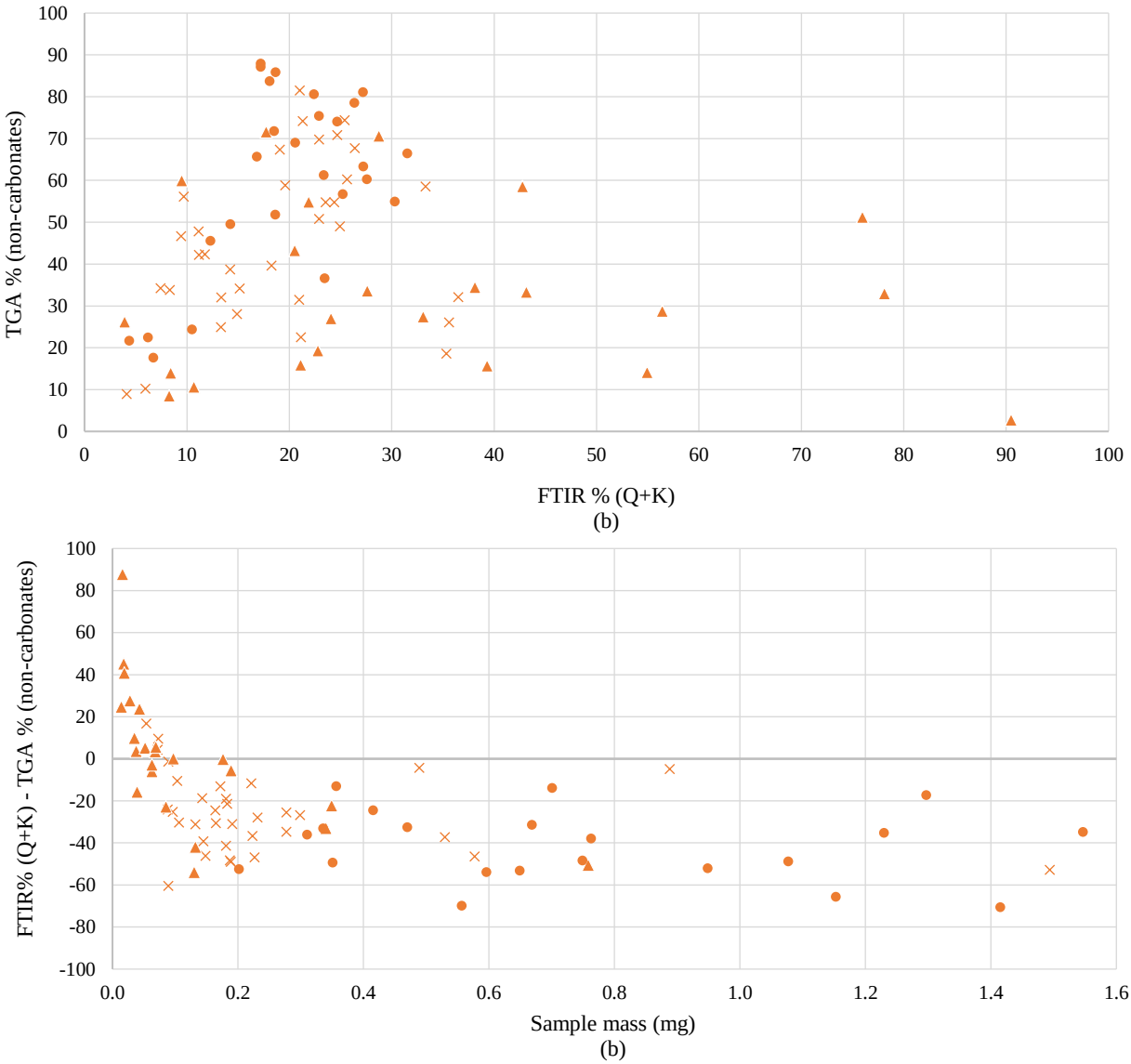

Figure 1-1. (a) Comparison of FTIR-based (Q+K) % versus TGA-based non-carbonate mineral mass % on corresponding PVC and PC replicate from each set collected in mines 10-25 (n=85). In 33 out of 93 samples, Q was below LOD, but K was above LOQ. (b). Difference between FTIR-based Q+K and TGA-based non-carbonate mineral mass % versus dust mass on each PVC replicate (n=83). The x-axis is capped at 1.6 mg since most of the data points are clustered in this range; 5 more data points exist between 1.6 - 8 mg, all following the observed trend. In both figures, ✕ = either Q or K below LOD, ▲ = either Q or K between LOD and LOQ; ● = both K and Q above LOQ.

Figure 1-1 (b) also clearly shows that low sample mass is correlated with observations of the FTIR result being higher than the TGA result. This is likely to be at least partly due to decreased analytical accuracy—and it is noteworthy that most of the low-mass samples in this study came from the intake and feeder locations (per Table 1-3). Based on SEM-EDX data, these samples often have relatively high carbonate (CB), coal and/or diesel particulate (C+MC) content, and thereby relatively low non-carbonate mineral content (ASK+ASO+S+SLO+M).

3.2 Comparison of the FTIR and TGA to particle-based SEM-EDX

Figure 1-2 shows the comparison between the FTIR and SEM-EDX results. As expected, results for FTIR derived Q and SEM-EDX derived S are in reasonable agreement (i.e., mean difference of about ±5%, with the exception of one outlier). That said, all but the outlier sample had <25% Q/S per either method, so the visual similarities between the two data series (in Figure 1-2) should be viewed accordingly.

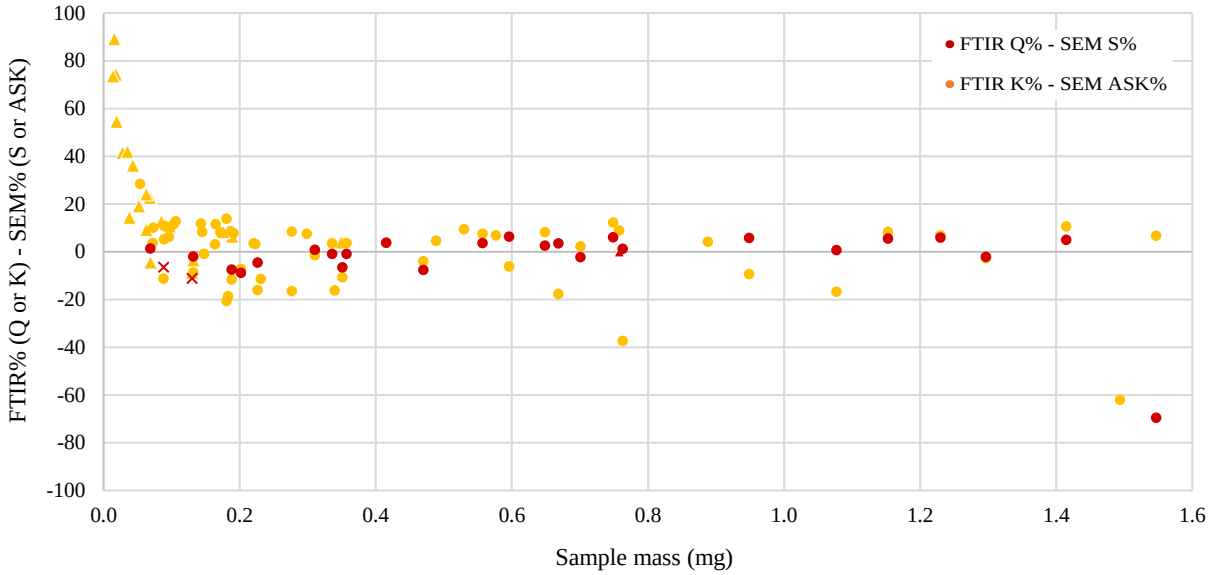

Figure 1-2. Difference between FTIR and SEM-EDX-derived mass % estimates for quartz/silica and kaolinite/alumino-silicates-kaolinite versus dust mass on each PVC replicate (n=33 for Q%-S%, n=83 for K%-ASK%). The x-axis is capped at 1.6 mg; 10 more data points exist (5 each for Q and K) between 1.6 - 8 mg, all following the observed trend. ✕ = below LOD, ▲ = between LOD and LOQ; ● = above LOQ.

Similar to the Q/S results, Figure 1-2 shows that FTIR K and SEM-EDX ASK results generally agree (mean difference of about 15%). Unlike the Q/S %, the K/ASK % ranged from ~0% up to ~90% per either method, so a mean difference of 15% can be considered to represent a good agreement. Similar to the comparison between FTIR and TGA, trends with sample mass are evident, with the lowest-mass samples likely being affected by accuracy issues. Considering there is reasonable agreement in K/ASK%, and ASK % is, on average, one-fourth of the total AS (i.e., ASK+ASO) per Table 1-3, it can be inferred there is indeed an abundance of non-kaolinite alumino-silicates in many of the samples. However, given the particle-based nature of the SEM-EDX analysis and the inordinately high AS content observed in many samples as mass increases, it is worth considering that other factors could be at play.

Figure 1-3 shows the comparison between the TGA and SEM-EDX results. In this case, all three primary components of the dust estimated by TGA (i.e., coal, carbonate, and non-carbonates) can be compared with results from SEM-EDX since its mineralogy classes can be loosely collapsed to match the TGA outputs per Table 1-1. The largest differences are again seen for the lowest-mass samples (typically in the I and F locations, per Table 1-3). Figure 1-3 suggests that these discrepancies are most often related to a tendency for the TGA to measure more coal (possibly including very fine diesel particulates not accurately counted in the SEM work) and less

carbonate (possibly overcounted in the SEM work due to its coarser size, see Sarver et al. 2019) versus the SEM-EDX.

However, the effect of sample mass in Figure 1-3 is visibly diminished above about 100 µg. After that, in general, the SEM-EDX still tends overpredict non-carbonate minerals (mostly ASK+ASO+S per Table 1-3) versus the comparative measure, but to a lesser extent than observed in Figure 1-2. Frequently, this overprediction of non-carbonates by the SEM-EDX corresponds with an underprediction of coal (C+MC). Possible explanations for these results could be that coal particles are either impure, or are being coated (i.e., occluded) by relatively fine alumino-silicates, especially in the sampling locations where dust is actively being generated. Since the SEM-EDX effectively classifies particles based on their elemental content, whereas TGA classifies particles based on their mass, such occurrences could lead to significant differences between dust compositions indicated by these two methods. Notably, the fact that the carbonate results in Figure 1-3 (like the Q/S results in Figure 1-2) are in relatively good agreement provides some indication that high sample mass is probably not the only reason for high ASK+ASO content per SEM-EDX—meaning that particle interference effects due to loading are not alone responsible.

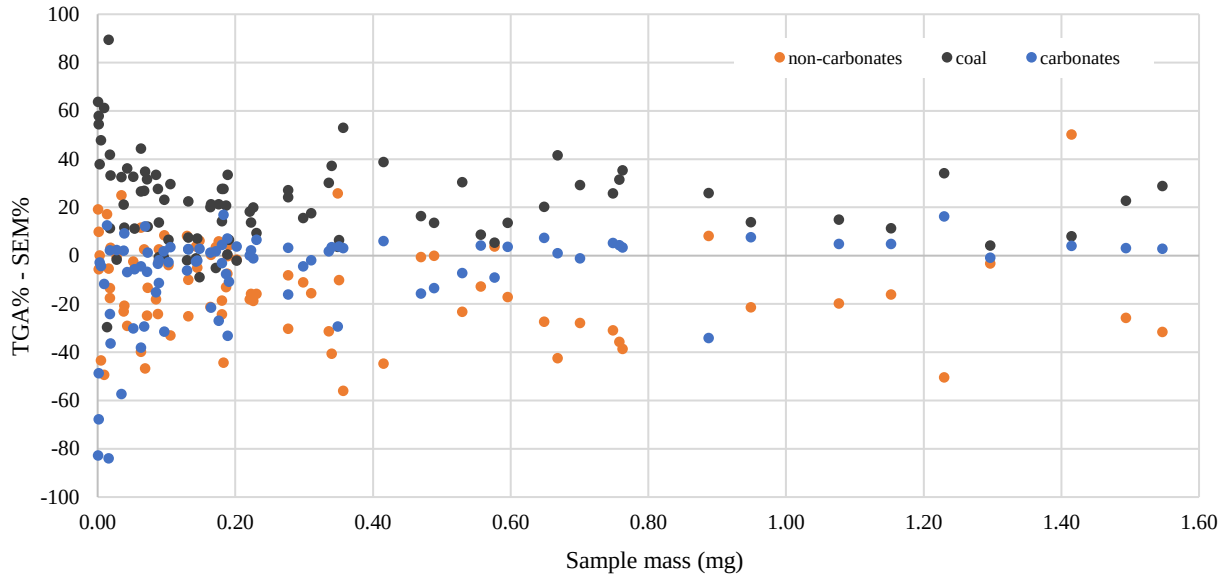

Figure 1-3. Difference between estimates of coal, carbonates, and non-carbonates mineral fractions derived from TGA and SEM-EDX results versus dust mass collected on each PVC replicate (n=91). The x-axis is capped at 1.6 mg; 5 sets of data points exist between 1.6 - 8 mg, all roughly following the observed trend.

4. CONCLUSIONS

For the first time, this study compared mineral content in respirable coal mine dust samples measured by FTIR, TGA, and SEM-EDX. Comparison of results from all three methods suggests the presence of significant non-carbonate mineral content other than quartz and kaolinite in the mine dust. Detailed analysis of the FTIR transmission and SEM-EDX elemental spectra might be valuable to better understand the specific mineral constituents. Further, results showed that the particle-based SEM-EDX frequently indicates much more mineral content (primarily other alumino-silicates) than is predicted by either of the mass-based measures. While sample mass/particle loading effects may be partly to blame, another possibility is that the SEM-EDX results are associated with impurity or occlusion of coal (or other particles) by fine alumino-silicates. While such particles may exhibit sufficient Si and Al to be classified as alumino-silicates

by the SEM-EDX, their mass may be dominated by coal, resulting in very little accounting to the corresponding TGA and FTIR measures (non-carbonates and kaolinite, respectively).

Aside from comparison of results between analytical methods, this study also demonstrated the application of NIOSH's new DOF-FTIR method for research purposes—as opposed to personal exposure monitoring as it has been primarily intended. Results illustrate the usefulness of this method, specifically for determination of kaolinite content along with quartz, and should support continuing efforts to integrate the method into research and engineering studies.

REFERENCES

Agioutanti, E., Keles, C., & Sarver, E. (2020). A thermogravimetric analysis application to determine coal, carbonate, and non-carbonate minerals mass fractions in respirable mine dust. *J Occup Environ Hyg*, *17*(2-3), 47-58. https://doi.org/10.1080/15459624.2019.1695057

Almberg, K. S., Halldin, C. N., Blackley, D. J., Laney, A. S., Storey, E., Rose, C. S., Go, L. H. T., & Cohen, R. A. (2018). Progressive Massive Fibrosis Resurgence Identified in U.S. Coal Miners Filing for Black Lung Benefits, 1970-2016. *Ann Am Thorac Soc*, *15*(12), 1420-1426. https://doi.org/10.1513/AnnalsATS.201804-261OC

Ashley, E. L., Cauda, E., Chubb, L. G., Tuchman, D. P., & Rubinstein, E. N. (2020). Performance Comparison of Four Portable FTIR Instruments for Direct-on-Filter Measurement of Respirable Crystalline Silica. *Ann Work Expo Health*, *64*(5), 536-546. https://doi.org/10.1093/annweh/wxaa031

Blackley, D. J., Crum, J. B., Halldin, C. N., Storey, E., & Laney, A. S. (2016). *Resurgence of Progressive Massive Fibrosis in Coal Miners* (Morbidity and Mortality Weekly Report, Issue.

Castranova, V., & Vallyathan, V. (2000). Silicosis and coal workers' pneumoconiosis. *Environ Health Perspect*, *108 Suppl 4*(suppl 4), 675-684. https://doi.org/10.1289/ehp.00108s4675

Cauda, E., Miller, A., & Drake, P. (2016). Promoting early exposure monitoring for respirable crystalline silica: Taking the laboratory to the mine site. *J Occup Environ Hyg*, *13*(3), D39-45. https://doi.org/10.1080/15459624.2015.1116691

CDC. (2006). *Advanced Cases of Coal Workers' Pneumoconiosis --- Two Counties, Virginia* (MMWR 55, Issue.

IARC. (1997). *Monographs on the evaluation of carcinogenic risks to humans: silica, some silicates, coal dust and para-aramid fibrils.* (Vol. 68).

Johann-Essex, V., Keles, C., Rezaee, M., Scaggs-Witte, M., & Sarver, E. (2017). Respirable coal mine dust characteristics in samples collected in central and northern Appalachia. *International Journal of Coal Geology*, *182*, 85-93. https://doi.org/10.1016/j.coal.2017.09.010

Johann-Essex, V., Keles, C., & Sarver, E. (2017). A Computer-Controlled SEM-EDX Routine for Characterizing Respirable Coal Mine Dust. *Minerals*, *7*(1), 15. https://doi.org/10.3390/min7010015

Laney, A. S., & Weissman, D. N. (2014). Respiratory diseases caused by coal mine dust. *J Occup Environ Med*, *56 Suppl 10*, S18-22. https://doi.org/10.1097/JOM.0000000000000260

Lee, T., Chisholm, W. P., Kashon, M., Key-Schwartz, R. J., & Harper, M. (2013). Consideration of kaolinite interference correction for quartz measurements in coal mine dust. *J Occup Environ Hyg*, *10*(8), 425-434. https://doi.org/10.1080/15459624.2013.801819

Miller, A. L., Drake, P. L., Murphy, N. C., Cauda, E. G., LeBouf, R. F., & Markevicius, G. (2013). Deposition Uniformity of Coal Dust on Filters and Its Effect on the Accuracy of FTIR Analyses for Silica. *Aerosol Sci Technol*, *47*(7), 724-733. https://doi.org/10.1080/02786826.2013.787157

Miller, A. L., Drake, P. L., Murphy, N. C., Noll, J. D., & Volkwein, J. C. (2012). Evaluating portable infrared spectrometers for measuring the silica content of coal dust. *J Environ Monit*, *14*(1), 48-55. https://doi.org/10.1039/c1em10678c

Miller, A. L., Weakley, A. T., Griffiths, P. R., Cauda, E. G., & Bayman, S. (2017). Direct-on-Filter alpha-Quartz Estimation in Respirable Coal Mine Dust Using Transmission Fourier Transform Infrared Spectrometry and Partial Least Squares Regression. *Appl Spectrosc*, *71*(5), 1014-1024. https://doi.org/10.1177/0003702816666288

MSHA. (2008). *Method No. P-7*.

NASEM. (2018). *Monitoring and Sampling Approaches to Assess Underground Coal Mine Dust Exposures*. The National Academies Press. https://doi.org/doi:10.17226/25111

NIOSH. (2019). *FAST (Field Analysis of Silica Tool)*. In (Version Build 1.0.7.2) NIOSH-CDC. https://www.cdc.gov/niosh/mining/works/coversheet2056.html

Sarver, E., Keles, C., & Rezaee, M. (2019). Beyond conventional metrics: Comprehensive characterization of respirable coal mine dust. *International Journal of Coal Geology*, *207*, 84-95. https://doi.org/10.1016/j.coal.2019.03.015

Schatzel, S. J. (2009). Identifying sources of respirable quartz and silica dust in underground coal mines in southern West Virginia, western Virginia, and eastern Kentucky. *International Journal of Coal Geology*, *78*(2), 110-118. https://doi.org/10.1016/j.coal.2009.01.003

Su, X., Ding, R., & Zhuang, X. (2020). Characteristics of Dust in Coal Mines in Central North China and Its Research Significance. *ACS Omega*, *5*(16), 9233-9250. https://doi.org/10.1021/acsomega.0c00078

Chapter 2 – Direct-on-filter FTIR Spectroscopy to estimate calcite as a proxy for limestone 'rock dust' in respirable coal mine dust samples

Nishan Pokhrel, Cigdem Keles, Lizeth Jaramillo, Eleftheria Agioutanti, and Emily Sarver

Citation: Pokhrel, N., Keles, C., Jaramillo, L., Agioutanti, E., & Sarver, E. (2021). Direct-on-Filter FTIR Spectroscopy to Estimate Calcite as a Proxy for Limestone 'Rock Dust' in Respirable Coal Mine Dust Samples. Minerals, 11(9), 922. https://www.mdpi.com/2075-163X/11/9/922

ABSTRACT

Application of fine, inert 'rock dust' (RD) to the surfaces in underground coal mines is a common method for mitigating coal dust explosion hazards. However, due to its size, RD has the potential to contribute to the respirable coal mine dust (RCMD) concentration. Though the RD component of RCMD does not appear to pose the sort of health hazards associated with other components such as crystalline silica, understanding its relative abundance may be quite helpful for evaluating and controlling primary dust sources. Given that RD products are frequently comprised of high-purity limestone (i.e., primarily calcite mineral), calcite may serve as a suitable proxy for measuring RD. To estimate the mass percentage of calcite in RCMD samples, this study demonstrates the successful application of direct-on-filter (DOF) Fourier-transform infrared (FTIR) spectroscopy. Incidentally, DOF FTIR has been the focus of recent efforts to enable rapid measurement of crystalline silica in RCMD. Concurrent measurement of other constituents such as calcite is thus a logical next step, which can allow a broader interpretation of dust composition and source contributions.

1. INTRODUCTION

Underground coal mining activities produce fine combustible coal dust. When present with methane—a gas naturally released from coal seams—there is a devastating risk of coal mine explosions (Luo et al., 2017; Man & Teacoach, 2009). It is well established that the use of inert 'rock dust' (RD) products can effectively prevent coal dust from taking part in such explosions (Cashdollar et al., 2010). During an explosion, the RD disperses, mixes with the coal dust, and prevents propagation of the flame front by acting as a heat sink (Cashdollar et al., 2010; Harris, 2009).

The practice of RD application to coal mine surfaces dates back more than a century, and federal regulatory requirements for rock dusting in US mines were included in the Coal Mine Safety and Health Act (1969) (MSHA, 1969). The regulation covers both application practices and product specifications. Although a variety of materials might be used to generate RD (e.g., dolomite, gypsum, anhydrite, shale, adobe), most products are comprised of pulverized, high-purity limestone (i.e., natural calcite or calcium carbonate, CaCO3) since it is inexpensive and widely available. In addition to being inert, RD products must also have relatively fine particle size to effectively mitigate coal dust explosion (Harris et al., 2015).

A joint survey by NIOSH and MSHA showed that there has been an increase in the fine coal dust in US coal mines over the past several decades, possibly due to an increase in mechanization (Cashdollar et al., 2010). Since finer coal dust has more surface area, it requires the application of more RD to inert (Harris et al., 2015). This, along with an increased focus on limiting

respirable coal mine dust (RCMD) exposure, has prompted questions regarding the contribution of RD to the overall RCMD concentration and the possible implications for occupational health (Harris et al., 2015; NASEM, 2018).

While acute exposure to calcite dust has not been shown to induce significant cytotoxicity, respiratory irritation is possible which might contribute to a higher risk of chronic obstructive pulmonary disease (COPD) (CDC, 1995; Khaliullin et al., 2019; NASEM, 2018). That said, whenever health effects due to RD products have been reported, the respirable crystalline silica (RCS) content was proposed to be the most likely cause (Khaliullin et al., 2019). It is noted that United States regulation does allow for a small percentage of respirable crystalline silica (RCS) in RD products (≤4% by mass, per 30CFR § 75.2), but studies have consistently indicated that common products typically do not exceed the standard (Colinet & Listak, 2012; Johann-Essex, Keles, Rezaee, et al., 2017; NASEM, 2018; Soo et al., 2016).

Still, if RD is significantly contributing to the RCMD concentration, this information is important to the overall understanding of dust sources and possible risks. For example, given equal exposure concentration and time, RCMD that is mostly sourced from limestone RD application likely presents less risk than RCMD that is mostly sourced from drilling into high-silica roof rock. Several recent studies have indicated that RD can indeed contribute to the RCMD concentration in some locations of underground mines (Johann-Essex, Keles, Rezaee, et al., 2017; Labranche et al., 2021; Pan et al., 2021; Phillips et al., 2017; Phillips et al., 2018; Sarver et al., 2019). These studies have relied on analytical methods such as scanning electron microscopy with energy dispersive X-ray (SEM-EDX) or thermogravimetric analysis (TGA) to investigate RCMD components. While valuable for research, such methods are simply not feasible for routine mine monitoring. Rather, methods are needed that can provide quick data on key RCMD components—enabling interpretation of dust sources and timely decision-making on interventions (NASEM, 2018).

A direct-on-filter (DOF) method that uses Fourier Transform Infrared (FTIR) Transmission Spectroscopy has been in development by the US National Institute for Occupational Safety and Health (NIOSH) for the measurement of RCS in RCMD samples (Cauda et al., 2016; Miller et al., 2013; Miller et al., 2012). Miller et al. showed a strong linear correlation (R-squared value of 0.90 - 0.97) between the DOF method and the standard MSHA P7 method for RCS analysis (Miller et al., 2012). In addition to RCS, though, this method can be used to estimate other minerals captured by the infrared spectra. Stach et al. combined data from transmission and diffuse reflectance infrared spectroscopy into a unified calibration model to estimate different minerals (such as alpha quartz, dolomite, and calcite) in real-world and lab-generated samples, expanding upon the current techniques that determine only alpha quartz (Stach et al., 2020). The potential to estimate kaolinite as a co-indicator of rock strata sourced dust (along with RCS) has recently been investigated (Pokhrel et al., 2021).

The current work aims to demonstrate the potential of the DOF FTIR method for estimating calcite as a proxy for RD in RCMD samples. To this end, RCMD samples from various locations in 16 underground mines were analyzed, along with laboratory-generated samples of respirable dust from primary source materials (e.g., RD products, raw coal, and rock strata) obtained from 15 of the 16 mines. The FTIR-derived calcite results are compared to estimations of the carbonate mineral fraction derived from TGA and SEM-EDX.

2. MATERIALS AND METHODS

A total of 93 sets of RCMD samples were collected from 16 underground coal mines in the United States (numbered as Mines 10-25, see Table 2-1). The sample sets were collected in key locations where RCMD source contributions were expected to vary based on nearby activities (Table 2-2); while an effort was made to sample all five locations in each mine, this was not always possible. Each set contained multiple samples that were collected simultaneously for about 2-4 h.

Table 2-1. Number and location of RCMD sample sets and dust source materials collected in the 16 underground coal mines included in this study. Descriptions of sampling locations are provided in Table 2-2.

Mine Number	Mining Method[1]	RCMD sample sets						Dust source materials				
		Sampling Location[2]					RCMD Total	Material[3]				Source material Total
		I	B	F	P	R		RD	C	RS	BD	
10	RP	1	2	2	2	1	8	-	-	1	1	2
11	RP	-	1	1	1	1	4	1	-	1	-	2
12	RP	1	1	-	1	1	4	1	1	1	-	3
13	LW	2	1	1	-	2	6	1	1	-	1	3
14	RP	1	1	1	1	-	4	1	1	1	1	4
15	RP	1	1	1	1	1	5	1	1	1	-	3
16	RP	-	1	1	1	1	4	1	1	-	1	3
17	LW	2	1	-	1	2	6	1	1	-	1	3
18	RP	1	1	1	1	1	5	1	1	1	1	4
19	RP	1	1	1	1	2	6	1	1	1	1	4
20	RP	1	1	2	1	1	6	1	-	-	1	2
21	RP	1	1	1	1	1	5	-	1	1	1	3
22	RP	1	-	1	1	-	3	1	1	1	1	4
23	LW	3	-	-	2	1	6	1	1	1	1	4
24	LW	3	-	1	-	2	6	1	-	-	1	2
25	RP	1	1	1	8	4	15	-	-	-	-	0
Total		20	14	15	23	21	**93**	13	11	10	12	**46**

[1] RP: Room and pillar method with continuous miner; LW: Longwall method.
[2] I: Intake; B: Roof bolter; F: Feeder; P: Production; R: Return
[3] RD: Rock dust; C: coal; RS: rock strata; BD: bolter dust.

Table 2-2. Description of the five key sampling locations within each mine.

Location	Description
Intake (I)	In the fresh airways, upstream of any bolting or mining activities
Roof bolter (B)	Just downwind of an active roof bolter
Feeder (F)	Adjacent to the feeder breaker, or along the main conveyor belt or transfer
Production (P)	Just downwind of an active continuous miner, or on the longwall face
Return (R)	In the exhaust airway, including downwind of ventilation tubing exhaust where

All sampling equipment and materials were obtained from Zefon International (Ocala, FL, USA). Sampling trains included a 10-mm nylon Dorr-Oliver cyclone and Escort ELF air pump (operated at 2.0 L/min to collect the respirable fraction of the airborne dust) to collect dust directly onto a 37-mm filter housed in a two-piece styrene cassette. In each sample set, at least three

samples were collected: one on a polyvinyl chloride (PVC) filter (5.0-µm pore size), and two on polycarbonate (PC) filters (track-etched with 0.4-µm pore size). The PVC filters were used for the DOF FTIR analysis and were pre- and post-weighed to determine the total sample mass using a microbalance (Sartorius MSE6.6S, Gottingen, Germany); the PC filters were used for TGA and SEM-EDX as described later.

At the time of RCMD sampling, bulk samples of primary dust source materials were also collected from 15 of the mines (Table 2-1). These include: the RD product being applied in the mine; run-of-mine coal (C) and rock strata (RS) materials that were pulled from the production belt; and material pulled from the roof bolter dust collection system (BD). In total, 46 source materials were collected, and these were used to generate respirable dust samples in the lab.

Since the bulk C and RS materials were very coarse (usually +5 cm), they were first pulverized and sieved to -230 mesh (-63 µm) to create a powder from which the respirable particles could be sampled; the RD and BD materials were already quite fine and required no preparation. To collect respirable dust from each source material, a small mass of the powdered material was aerosolized in a sealed enclosure using compressed air. The aforementioned sampling trains were used to collect samples (three on PVC filters and three on PC for each material) over durations of several minutes. Again, the PVC filters were pre- and post-weighed to determine the total sample mass.

2.1. Fourier Transform Infrared (FTIR) Analysis and Calibration

All available PVC filters (RCMD and lab-generated samples of dust source materials) were analyzed using a portable FTIR transmission instrument (ALPHA II, Bruker, Billerica, MA, USA). For this, the filter was carefully placed into a compatible four-piece cassette (Zefon International; Ocala, FL, USA), which was mounted onto a sample cradle and placed inside the instrument compartment so that the IR beam passed through the center of the filter (Chubb & Cauda, 2021). The absorbance spectrum was obtained from 16 scans of the central 6-mm diameter area of each filter at a resolution of 4 cm^{-1} in the spectral range of 4000 cm^{-1} to 400 cm^{-1}, using Blackman-Harris three-term apodization function. Raw spectra were then background corrected using Bruker's OPUS software (Version 8.2.28, 32 bit). The correction was done by subtracting the spectra of a blank PVC filter from that of the dust sample filter. A rubber band baseline correction with 64 baseline points was performed on the resultant spectra to remove distortions (Miller et al., 2012; Miller et al., 2017).

To determine calcite mass (µg) from a sample's FTIR spectra, a quantification model was developed using lab-generated samples of respirable sized particles of pure and natural calcite (CB Minerals LLC, Mamaroneck, NY, USA). A total of eight samples (~100-1200 µg) were prepared on pre- and post-weighed PVC filters using the same procedure as for the powdered mine dust source materials and then analyzed by FTIR as described above. In the IR spectra of pure calcite, one of its major characteristic peaks appears at ~877 cm^{-1} (Jones & Jackson, 1993). The OPUS software was used to calculate the integrated absorbance peak area in the spectral range of 890 to 865 cm^{-1}, which can be correlated to the calcite sample mass.Figure 2-1 shows the results for the pure calcite samples and supports a linear correlation between the integrated FTIR peak area and calcite mass (Equation 2-1):

Equation 2-1: $$Calcite\ mass\ (\mu g) = \frac{Absorbance\ peak\ area}{0.00334}$$

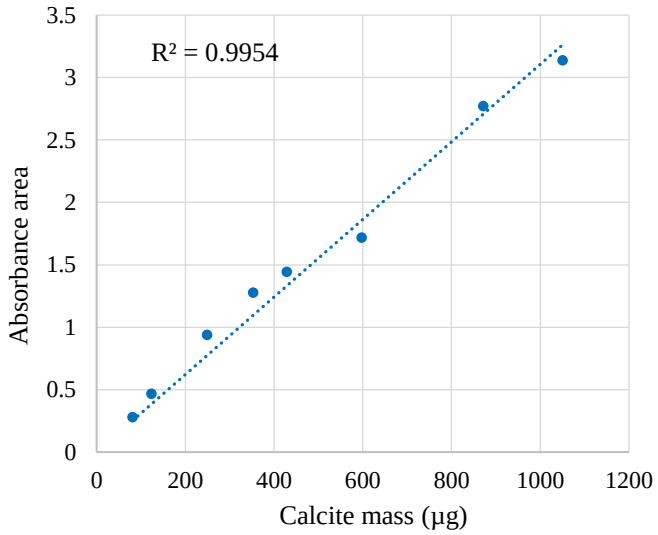

Figure 2-1. Calibration curve for the calcite quantification model prepared using eight respirable samples of respirable pure calcite. The Y-axis shows the integrated absorbance peak area for calcite (between 890 to 865 cm^{-1}) as a function of sample mass (µg) determined gravimetrically.

Following the collection of the FTIR spectra, Equation 2-1 was used to estimate the calcite mass (µg) in the lab-generated samples of dust source materials. Then, calcite mass was converted to calcite mass fraction (%) using the total dust sample mass. As mentioned, multiple PVC filters were collected for each source material, so the reported calcite results represent their average.

To estimate calcite mass in the RCMD samples, Equation 1 was slightly modified. This is because, unlike the lab-generated samples of dust source materials and pure calcite, the RCMD samples were collected in relatively low-concentration environments (and over longer sampling duration), which can affect the dust deposition pattern on the PVC filter. (I.e., Samples collected in high-concentration environments tend to have more center-heavy loading, which can slightly change the relationship between FTIR calcite peak area measured on the center of the filter and total calcite mass across the entire filter area). As such, Equation 2-1 was modified to Equation 2-2:

Equation 2-2:
$$Calcite\ mass\ (\mu g) = \frac{F_{lab}}{F_{RCMD}} \times \frac{Absorbance\ peak\ area}{0.00334}$$

where $\frac{F_{lab}}{F_{RCMD}}$ is the ratio of the calibration factors determined for RCS in sampling environments representative of the lab sampling conducted in the current study and RCMD sampling. F_{RCMD}=0.00465 and was previously established by NIOSH using pure quartz calibration samples collected in a calm air dust chamber with low concentration (Cauda et al., 2016). F_{lab}=0.00695 and was developed by the authors of the current study using a similar quartz material as NIOSH, but the samples were collected in the same manner and high concentration enclosure described above for pure calcite and mine dust source materials.

For the FTIR instrument used here, the limits of detection (LOD) and quantification (LOQ) for calcite were estimated to be ~1 µg and ~3 µg, respectively, using the standard deviation of the calcite peak measurement of 20 blank PVC filters.

2.2. Thermogravimetric Analysis (TGA)

TGA was used to analyze one PC filter from each of the 93 RCMD and 46 lab-generated sample sets. TGA is a mass-based method that can be used to estimate the coal, carbonate, and non-carbonate mineral fractions in a dust sample, and these fractions can be loosely correlated with the primary dust sources in many coal mines (i.e., the coal strata, RD products, and rock strata, respectively). The TGA method has been described in detail by Agioutanti et al. (Agioutanti et al., 2020). Briefly, the dust was recovered from the PC filters by sonication in isopropyl alcohol, transferred to a clean tared pan, and analyzed by a Q500 Thermogravimetric Analyzer (TA Instruments, New Castle, DE, USA) using a specified thermal ramping routine. The TGA routine proceeds as follows: ramp from ambient to 200 °C (50 °C/min) and isotherm at 200 °C for 5 min; ramp to 480 °C (20 °C/min) and isotherm for 50 min; ramp to 800 °C (20 °C/min) and isotherm for 5 min. Based on the work by Agioutanti et al., the coal is expected to completely oxidize between 200 and 480 °C, and carbonates (modeled as calcite) should thermally decompose between 400 and 800 °C ($CaCO_3 \rightarrow CaO + CO_2$) [27]. Thus, the sample residue at the end of the TGA routine is assumed to be CaO + noncarbonate minerals. Then, a series of mass balance equations established by Agioutanti et al. was applied to apportion the dust to the three fractions specified above using the sample weight change in a few characteristic temperature regions (Agioutanti et al., 2020). It is noted here that the TGA method was developed using similar sampling sizes as the RCMD and dust source material samples analyzed for this study.

2.3. Scanning electron microscopy with energy dispersive X-ray (SEM-EDX)

One PC filter from each of the 93 RCMD and 46 lab-generated sample sets was also analyzed by SEM-EDX, which yielded data on particle size and mineralogy distributions. Sample preparation and analysis were done following the methods outlined by Sarver et al. (Sarver et al., 2019). Briefly, a 9-mm sub-section was carefully cut from each filter and sputter coated with Au/Pd. Then, it was analyzed using an FEI Quanta 600 FEG environmental SEM (Hillsboro, OR, USA) equipped with a backscatter electron detector BSD and a Bruker Quantax 400 EDX spectroscope (Ewing, NJ, USA). The analysis covered particles in the range of about 0.1-10 µm and included about 800 particles per sample.

Each particle's long and intermediate (perpendicular to long) dimensions were measured, and its elemental spectra were used to bin it into one of eight mineralogy classes per Table 2-3 or into an "other" class if it did not meet the criteria for one of the defined classes. Of relevance to the current study, the carbonate class (CB) is expected to be dominated by RD-sourced particles in many coal mines; the other classes are expected to contain coal (C, MC) and non-carbonate mineral particles (e.g., ASK, ASO, S) primarily sourced from cutting or drilling into the coal and surrounding rock strata, and possibly diesel particulates (included in C) in some mines (Johann-Essex, Keles, & Sarver, 2017; Sarver et al., 2019). Particle dimensions and classifications were used to estimate the mass fraction of dust in each class. This was done by first computing each particle's volume using the product of its projected area diameter and short dimension, based on an assumed ratio for the short-to-intermediate dimension (S:I) for each mineralogy class (i.e., where the short dimension is the height of the particle as it sits on the filter; Table 2-3). Then, the volume was multiplied by an assumed specific gravity, again based on the mineralogy class (Table 2-3). Finally, the computed particle masses were summed for each of the classes and divided by the total mass of particles in all classes for the sample.

Table 2-3. SEM-EDX classification criteria for sub- and supra-micron particles, along with assumptions for S:I ratio and SG for each mineralogy class (updated from Sarver et al. (Sarver et al., 2019)).

Class[1]	Routine	Normalized atomic % by element								Particle size to mass assumptions	
		C	O	Al	Si	Ca	Mg	Ti	Fe	S:I	SG
C	Sub Supra	≥75	<29	≤0.30	≤0.30	≤0.41	≤0.50	≤0.50 ≤0.06	≤0.50 ≤0.15	0.6	1.4
MC	Sub Supra			<0.44 <0.35	<0.44 <0.35	≤1.00 ≤0.50	≤0.50 ≤0.50	≤1.00 ≤0.60	≤1.00 ≤0.60	0.6	1.4
ASK[2]	Sub Supra			≥0.44, (≥37) ≥0.35, (≥39)	≥0.44, (≥42) ≥0.35, (≥32)	(<16) (<8)	(<4) (<15)	(<8) (<13)	(<10) (<13)	0.4	2.6
ASO[2]	Sub Supra			≥0.44, (<37) ≥0.35, (<39)	≥0.44, (<42) ≥0.35, (<32)	(≥16) (≥8)	(≥4) (≥15)	(≥8) (≥13)	(≥10) (≥13)	0.4	2.6
SLO[3]	Sub Supra				≥0.50 ≥0.33					0.4	2.6
S[4]	Sub Supra				≥0.50 ≥0.33					0.7	2.65
M	Sub Supra			>1.00				>1.00	>1.00	0.7	4.96
CB	Sub Supra	<88	>9			>1.00 >0.50	>0.50			0.7	2.7

[1] C: carbonaceous; MC: mixed carbonaceous; ASK: aluminosilicate-kaolinite; ASO: aluminosilicate-other; SLO: silicates-other; S: silica; M: heavy minerals; CB: carbonates.
[2] To differentiate ASK from ASO, additional limits for Al, Si, Ca, Mg, Ti, and Fe are shown in parenthesis (normalized to exclude C and O)
[3] Additional limits for SLO: Si/(Al+Si+Ca+Mg+Ti+Fe) < 0.5
[4] Additional limits for S: Al/Si < 1/3 and Si/(Al+Si+Ca+Mg+Ti+Fe) ≥ 0.5

3. RESULTS AND DISCUSSION

3.1 Dust source materials

As a proof-of-concept, Figure 2-2 presents results on the lab-generated respirable samples from all 46 dust source materials. (Data are available in Table A-2 in the Appendix.) As expected, all but one of the 13 RD material samples show very high fractions (>90%) of calcite per the FTIR analysis. These results are validated by the TGA- and SEM-EDX-derived carbonate mass fractions (Figure 2-2 (a) and (b), respectively), and the good agreement between all three methods suggests that most of the carbonate content in the samples is indeed calcite. For the one sample that shows only about 63% calcite, the higher TGA and SEM-EDX carbonate estimations (95 and 98%, respectively) indicate that this RD product also contained significant dolomite content (and indeed a significant peak corresponding to dolomite was observed on the FTIR spectra, though not quantified).

Notably, for two of the RD material samples, the FTIR actually indicates calcite mass fraction greater than 100%, which is practically impossible. This is likely due to particularly center-heavy dust loading on the filter samples generated for these two materials. As previously mentioned, the dust deposition pattern on the sample filter can influence the FTIR result; and while the sample collection procedure was the same for all lab-generated samples, it is possible that these RD materials had a slightly increased tendency for center loading relative to the pure and fine calcite samples used for calibration (Figure 2-1). For example, this could happen if the particle size distribution was relatively coarse. Nevertheless, even with some overestimation of the calcite % in these two materials, the FTIR results are still in good agreement with the TGA and SEM-

EDX (i.e., absolute difference of <11% in ~90% of sample pairs, with mean differences of ± 7.3 and ± 3.4%, respectively).

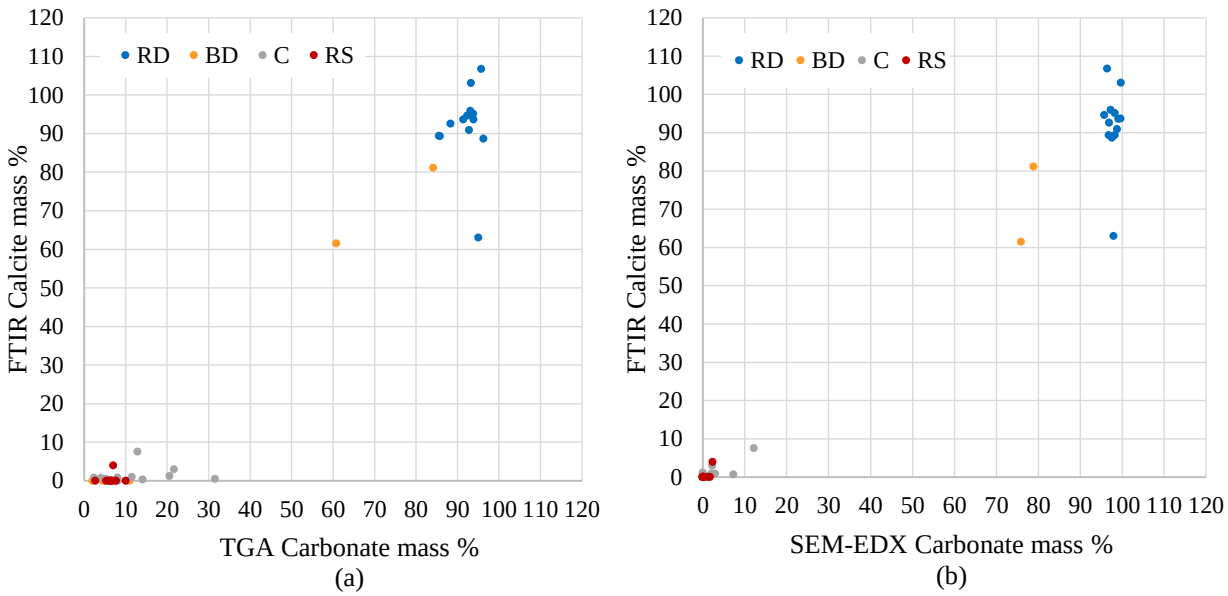

Figure 2-2. Comparison of FTIR-derived calcite % and (a) TGA- or (b) SEM-EDX-derived carbonate % for lab-generated respirable dust samples from RD, BD, C, and RS source materials (n = 46 each). In total, none of the 13 RD samples; 10 of the 12 BD samples; 1 of the 11 C samples; and 9 of the 10 RS samples had calcite mass less than LOD for the FTIR; none of the samples had calcite mass between LOD and LOQ.

For the other dust source materials, the FTIR results were also generally consistent with expectations (and the TGA and SEM-EDX results), with most of the C, RS, and BD samples showing very low calcite fractions. In fact, for many samples, the FTIR result was below the LOD or LOQ. Two BD samples (Mines 19 and 20) did show high calcite content (62 and 81%, respectively). This is attributed to the fact that the roof rock in these mines is characterized as limestone, whereas all other mines represented in this study had primarily shale, sandstone, and/or slate roof rock strata. Thus, while the calcite (or carbonate) fraction of RCMD is generally expected to be associated with RD application in the mine, exceptions are certainly possible.

It should also be mentioned that the TGA indicated significant carbonate content (>20%) in a few C material samples (Mines 13, 15, and 21), which disagreed with the corresponding FTIR and SEM-EDX results. However, upon inspection of the thermograms for those samples it was observed that the coal did not completely oxidize in the expected temperature range as it does for most coal materials—so the TGA method misclassified some coal as carbonates.

3.2 RCMD

Figure 2-3 presents the results for the RCMD samples (and data are tabulated in Table A-1). Again, comparisons are shown between the FTIR-derived calcite and the TGA- and SEM-EDX-derived carbonate fractions (Figure 2-3 (a) and (b), respectively). Overall, the results from the three methods generally trend together, though there is a lot of scatter in the data. Moreover, while the FTIR tends to overpredict the TGA, it tends to underpredict the SEM-EDX. Both of these observations can be attributed, at least in part, to the relatively low masses of many of the available RCMD samples. Of the 93 samples on PVC filters (i.e., on which the dust mass could be

accurately weighed), 51 had a mass <200 µg; and on 8 samples the mass was insufficient to conduct FTIR and/or TGA (i.e., n=85 in Figure 2-3).

Figure 2-4 illustrates, as a function of RCMD sample mass, the relative agreement between the FTIR and TGA or SEM-EDX results. For this plot, the ordinate (y) axis values represent the difference between FTIR calcite % — TGA or SEM-EDX carbonate % (e.g., for a sample that showed 23% calcite by FTIR and 17% carbonate by TGA, the plot shows 23% - 17% = 6%). There is much better agreement between the methods with increasing samples mass, which makes sense considering that the accuracy of both FTIR and TGA is mass-limited. For samples with mass >200 µg, the mean difference observed between the FTIR—TGA and FTIR—SEM-EDX results is just ±6.1% and ±3.4%, respectively. For relatively low mass samples, however, the over/underprediction trends in Figure 2-3 become clearer. All that said, it is worth noting that the RCMD samples included in this study have generally lower masses (due to short sampling times) than would be expected for full-shift RCMD samples (i.e., similar to what might be collected for the DOF-FTIR analysis of RCS that has been proposed by NIOSH).

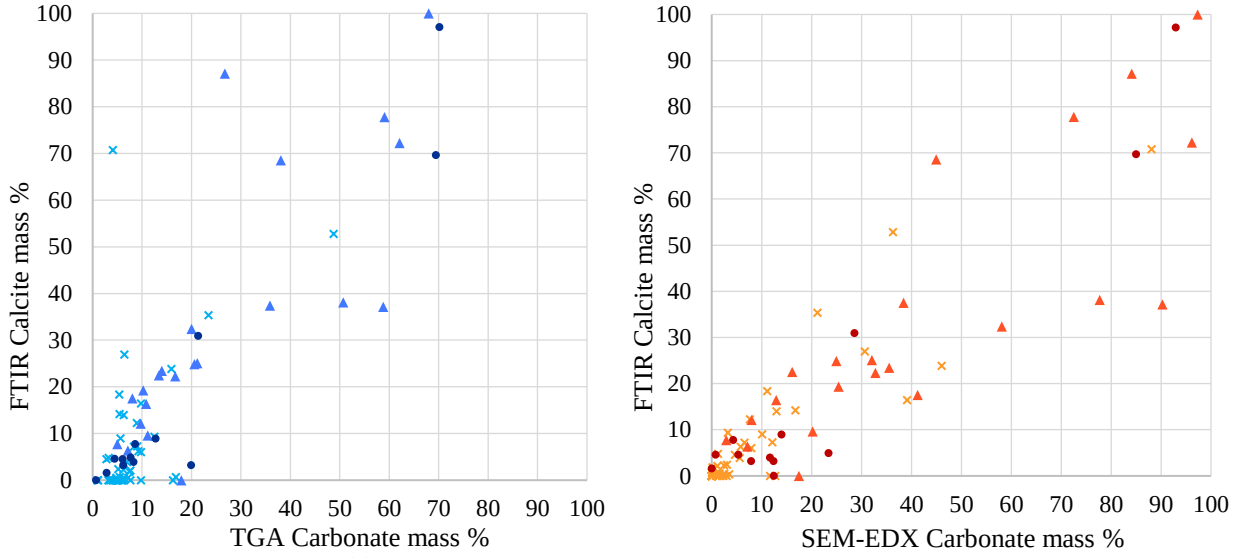

Figure 2-3. Comparison of FTIR-based calcite mass % and (a) TGA- or (b) SEM-EDX-based carbonate mineral mass % versus on corresponding PC and PVC filters from each sample set (n = 85 each). In the figures, × = FTIR calcite mass below LOD, ▲ = between LOD and LOQ; ● = above LOQ. In total, 37 of the 93 FTIR samples had calcite mass below the LOD, 28 samples were between LOD and LOQ, and 28 samples were above LOQ.

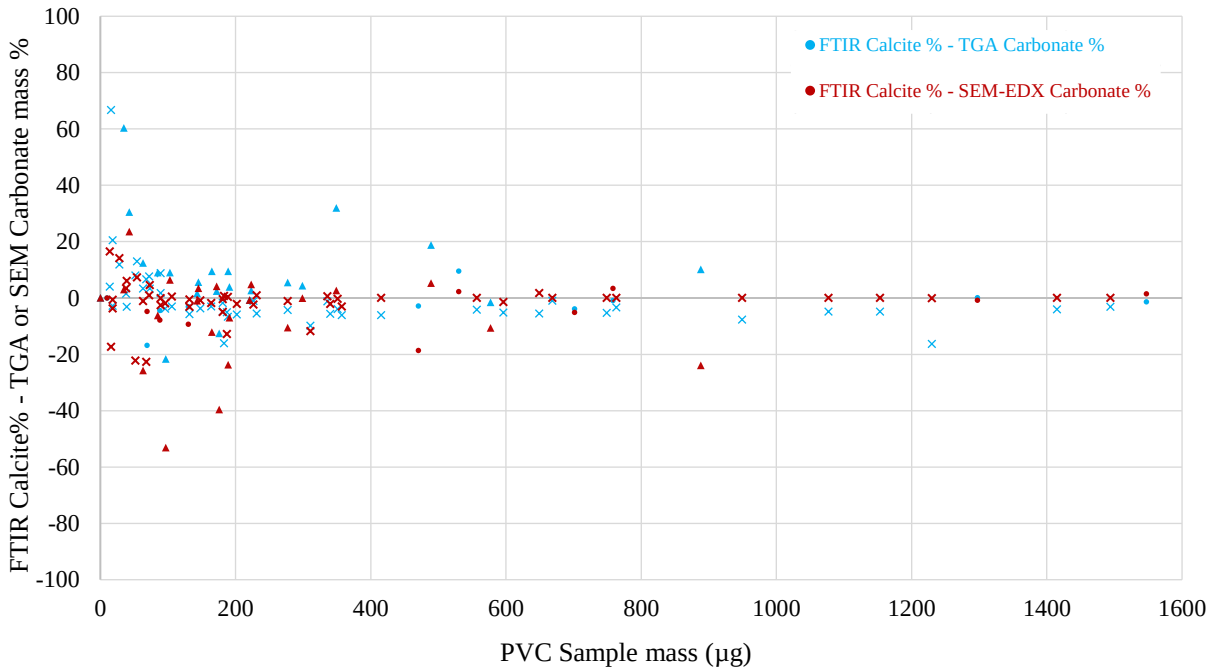

Figure 2-4. Difference between FTIR-based calcite mass % and TGA- or SEM-EDX-based carbonate mineral mass % versus sample mass on each PVC replicate sample collected in US underground coal mines (n = 85 for both). ✕ = FTIR calcite mass below LOD, ▲ = between LOD and LOQ; ● = above LOQ.

Figure 2-5 presents the FTIR, TGA, and SEM-EDX results with respect to the specific RCMD sampling locations. (Note that results from Mines 19 and 20 are excluded from the figure since limestone roof strata in these mines confounds the use of calcite/carbonate as a proxy for RD contribution to the RCMD.) The relatively wide discrepancies between results for intake and feeder samples are attributed to the typically low sample masses in these locations (18 out of 20 intake and 13 out of 15 feeder samples were <200 µg).

Both the FTIR and SEM-EDX suggest that RD contributes significantly to the RCMD in many intake samples. This is consistent with expectations since rock dusting is routinely performed in intake airways, which are also upwind of most other activities (e.g., roof bolting, coal/rock extraction, and crushing/handling that generate dust from the geologic strata in the mine) aside from traffic that can re-entrain dust. Results from all three methods additionally indicate that RD can sometimes contribute significantly to RCMD in the return airways. This is logical since the returns receive dust transported from all other airways in the mine, and these areas themselves may undergo further rock dusting.

On the other hand, the RD contribution to RCMD generally appears to be minor in the roof bolter, production, and feeder locations, which are expected to be more influenced by nearby activities that generate dust from the mine strata. Notable exceptions were the roof bolter sample from Mine 17 and the production sample from Mine 23, which show relatively high calcite/carbonate fractions across all three analytical methods. Given that only the RD materials from these mines showed high calcite/carbonate, the results suggest that rock dusting upwind of the sampling locations did indeed contribute significantly to the RCMD. Indeed, extensive RD application was observed in the Mine 23 intake airway just upwind of the production face during the collection of the production and return samples, which showed ~89 and ~63% calcite,

respectively. (The intake sample in Mine 23 was collected during an earlier shift when active RD application was not observed, and it showed only ~33% calcite.)

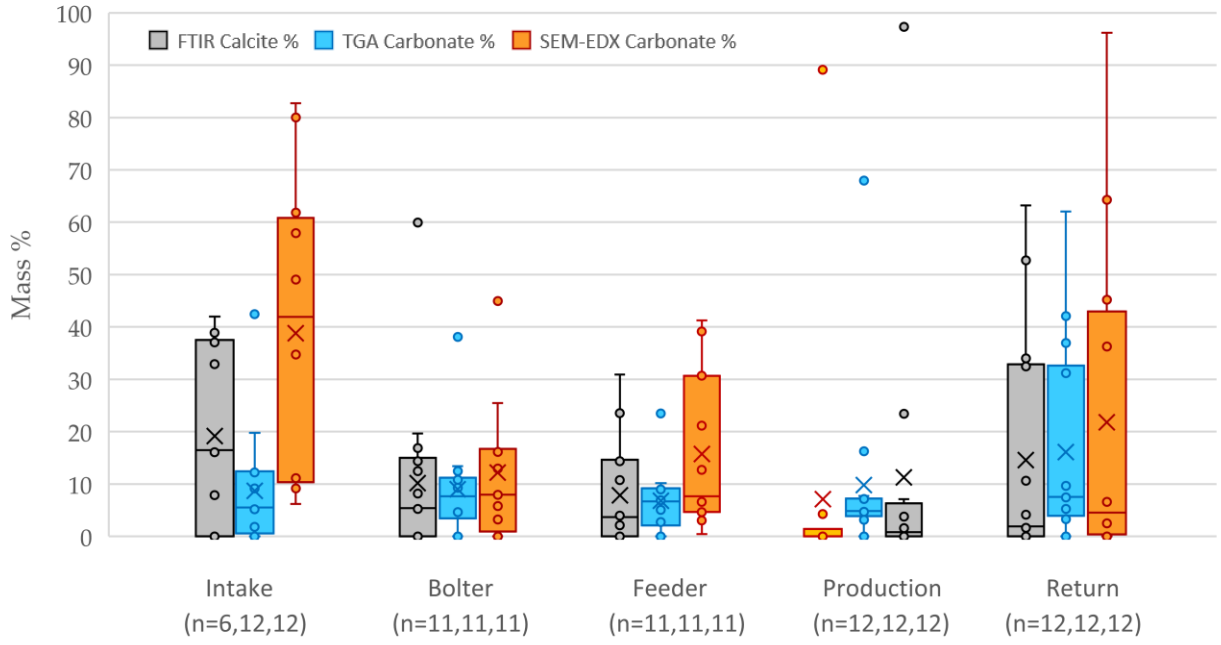

Figure 2-5. Box and whisker plot showing the FTIR, TGA, and SEM-EDX derived calcite/carbonate mass % for RCMD samples collected in each sampling location (excluding samples from Mines 19 and 20). In some mines, multiple sample sets were collected in a particular location (see Table 2-1); to avoid biasing results toward these mines, the multiple sample values were averaged to yield a single mine x location value. Thus, n values show the number of data points available for each unique sampling location. Lower, middle, and upper box boundaries show the 25th, 50th, and 75th quartiles, respectively; lower and upper whisker lines show the lowest and highest values, respectively—except the outliers (defined as points 1.5 times the interquartile range away from the box boundaries); circles show the individual data points, and ✕ marks the mean calcite/carbonate mass %.

While active rock dusting was not always observed during RCMD sampling, the general appearance of mine floors and ribs provided anecdotal evidence that the larger longwall mines (as opposed to smaller mines using room and pillar methods with continuous miners) represented in this study were more frequently and extensively rock dusted. Accordingly, the RCMD samples collected in these mines tended to show higher calcite/carbonate content across all sampling locations (Table 2-4). This is especially evident for the production and return locations. Although generalization of these results is not advisable due to the relatively small number of longwall mine samples included in this study, it can be noted that the longwalls represented here were observed to have particularly effective dust controls at the production face (i.e., ventilation, water sprays on the longwall shearer that minimized RCMD from the coal/roof rock extraction).

Table 2-4. FTIR mean calcite mass % and standard deviation (SD) for RCMD samples (excluding Mines 19 and 20) grouped by sampling locations and mining method. As for Figure 2-5, results were averaged in cases where multiple samples were available in the same mine x location.

	Room and Pillar			Longwall		
Sampling Location	**Mean**	**SD**	**n**	**Mean**	**SD**	**n**
Intake	13.7	6.6	2	36.8	12.4	4
Bolter	10.5	8.1	9	34.3	48.5	2
Feeder	10.3	12.5	9	17.0	0.8	2
Production	1.2	2.4	10	48.7	68.1	2
Return	3.1	3.9	8	52.1	17.0	4

4. CONCLUSIONS

Portable FTIR spectroscopy can enable rapid, direct-on-filter (DOF) analysis of respirable coal mine dust (RCMD) samples. While the primary focus of such analysis has been on the measurement of crystalline silica, the potential exists for concurrent measurement of other dust constituents too. These include calcite (calcium carbonate), which is the predominant constituent in many limestone rock dust (RD) products that are applied in coal mines to mitigate explosibility hazards.

Analysis of respirable dust generated from primary dust source materials from 15 underground coal mines across the United States indicated that RD products were the major source of respirable calcite in 13 mines. In such situations, calcite may thus serve as a suitable proxy for the RD contribution to RCMD. However, in the two mines studied here, the roof rock was dominated by limestone which would confound efforts to use calcite as a proxy for RD in RCMD. As such, a survey of primary dust source materials in any particular mine should be a critical precursor to the interpretation of RCMD results.

With respect to the quality of DOF FTIR measurement of calcite in respirable dust samples, results demonstrated good agreement with other methods (TGA and SEM-EDX)—especially for samples with sufficient total dust mass. Moreover, results were generally consistent with expectations based on the sample source or conditions in the specific mine sampling location. It is noted that no effort was made here to investigate the possible analytical confounders, such as the effects/interferences for calcite in the FTIR spectra due to the mixture of various mineral components in the RCMD samples; though this may be an issue in specific instances and is deserving of attention moving forward. As mentioned earlier, due to the nature of the quantification model, the dust deposition pattern influences the FTIR results. Results suggest that for more accurate quantification, the particle size distribution of calibration samples and samples for analysis should be somewhat similar, which then translates to a similar dust deposition pattern.

Overall, the findings from this study indicate that DOF FTIR can indeed be used to estimate calcite as a proxy for RD in RCMD in many coal mines. Such information may be quite valuable in view of dust source apportionment or tracking spatial and temporal changes in mine conditions.

REFERENCES

Agioutanti, E., Keles, C., & Sarver, E. (2020). A thermogravimetric analysis application to determine coal, carbonate, and non-carbonate minerals mass fractions in respirable mine dust. *J Occup Environ Hyg*, *17*(2-3), 47-58. https://doi.org/10.1080/15459624.2019.1695057

Cashdollar, K. L., Sapko, M. J., Weiss, E. S., Harris, M. L., Man, C. K., Harteis, S. P., & Green, G. M. (2010). *Recommendations for a New Rock Dusting Standard to Prevent Coal Dust Explosions in Intake Airways*. Pittsburgh, PA: NIOSH

Cauda, E., Miller, A., & Drake, P. (2016). Promoting early exposure monitoring for respirable crystalline silica: Taking the laboratory to the mine site. *J Occup Environ Hyg*, *13*(3), D39-45. https://doi.org/10.1080/15459624.2015.1116691

CDC. (1995). *Occupational Safety and Health Guideline for Calcium Carbonate*.

Chubb, L. G., & Cauda, E. G. (2021). A novel sampling cassette for field-based analysis of respirable crystalline silica. *Journal of Occupational and Environmental Hygiene*, *18*(3), 103-109. https://doi.org/10.1080/15459624.2020.1868481

Colinet, J. F., & Listak, J. M. (2012). Silica and respirable content in rock dust samples. *Coal Age*, *117*, 48-52.

Harris, M. L., Sapko, M. J., Zlochower, I. A., Perera, I. E., & Weiss, E. S. (2015). Particle size and surface area effects on explosibility using a 20-L chamber. *Journal of Loss Prevention in the Process Industries*, *37*, 33-38. https://doi.org/10.1016/j.jlp.2015.06.009

Harris, M. L. C., K.L.; Man, C.K.; Thimons, E. (2009, November 10-13, 2009). *Mitigating coal dust explosions in modern underground coal mines.* Ninth International Mine Ventilation Congress, New Delhi, India. https://www.cdc.gov/niosh/mining/UserFiles/works/pdfs/mcdei.pdf

Johann-Essex, V., Keles, C., Rezaee, M., Scaggs-Witte, M., & Sarver, E. (2017). Respirable coal mine dust characteristics in samples collected in central and northern Appalachia. *International Journal of Coal Geology*, *182*, 85-93. https://doi.org/10.1016/j.coal.2017.09.010

Johann-Essex, V., Keles, C., & Sarver, E. (2017). A Computer-Controlled SEM-EDX Routine for Characterizing Respirable Coal Mine Dust. *Minerals*, *7*(1), 15. https://doi.org/10.3390/min7010015

Jones, G. C., & Jackson, B. (1993). *Infrared Transmission Spectra of Carbonate Minerals*. Springer-Science+Business Media, B.V. https://doi.org/https://doi.org/10.1007/978-94-011-2120-0

Khaliullin, T. O., Kisin, E. R., Yanamala, N., Guppi, S., Harper, M., Lee, T., & Shvedova, A. A. (2019). Comparative cytotoxicity of respirable surface-treated/untreated calcium carbonate rock dust particles in vitro. *Toxicol Appl Pharmacol*, *362*, 67-76. https://doi.org/10.1016/j.taap.2018.10.023

Labranche, N., Keles, C., Sarver, E., Johnstone, K., & Cliff, D. (2021). Characterization of Particulates from Australian Underground Coal Mines. *Minerals*, *11*(5), 447. https://doi.org/10.3390/min11050447

Luo, Y., Wang, D., & Cheng, J. (2017). Effects of rock dusting in preventing and reducing intensity of coal mine explosions. *International Journal of Coal Science & Technology*, *4*(2), 102-109. https://doi.org/10.1007/s40789-017-0168-z

Man, C., & Teacoach, K. A. (2009). How does limestone rock dust prevent coal dust explosions in coal mines? 2009 SME Annual Meeting and Exhibit, Denver, Colorado.

Miller, A. L., Drake, P. L., Murphy, N. C., Cauda, E. G., LeBouf, R. F., & Markevicius, G. (2013). Deposition Uniformity of Coal Dust on Filters and Its Effect on the Accuracy of FTIR Analyses for Silica. *Aerosol Sci Technol*, *47*(7), 724-733. https://doi.org/10.1080/02786826.2013.787157

Miller, A. L., Drake, P. L., Murphy, N. C., Noll, J. D., & Volkwein, J. C. (2012). Evaluating portable infrared spectrometers for measuring the silica content of coal dust. *J Environ Monit*, *14*(1), 48-55. https://doi.org/10.1039/c1em10678c

Miller, A. L., Weakley, A. T., Griffiths, P. R., Cauda, E. G., & Bayman, S. (2017). Direct-on-Filter alpha-Quartz Estimation in Respirable Coal Mine Dust Using Transmission Fourier Transform Infrared Spectrometry and Partial Least Squares Regression. *Appl Spectrosc*, *71*(5), 1014-1024. https://doi.org/10.1177/0003702816666288

Federal Coal Mine Health and Safety Act, (1969). https://arlweb.msha.gov/solicitor/coalact/69act.htm

NASEM. (2018). *Monitoring and Sampling Approaches to Assess Underground Coal Mine Dust Exposures*. The National Academies Press. https://doi.org/doi:10.17226/25111

Pan, L., Golden, S., Assemi, S., Sime, M. F., Wang, X., Gao, Y., & Miller, J. (2021). Characterization of Particle Size and Composition of Respirable Coal Mine Dust. *Minerals*, *11*(3), 276. https://doi.org/10.3390/min11030276

Phillips, K., Keles, C., Scaggs-Witte, M., Johann-Essex, V., Rezaee, M., & Sarver, E. (2017). *Applications of thermal and laser-based methods for monitoring airborne particulates in coal mines* Virginia Polytechnic Institute and State University]. Blacksburg, VA.

Phillips, K., Keles, C., Scaggs-Witte, M., & Sarver, E. (2018). Coal and mineral mass fractions in personal respirable dust samples collected by central appalachian miners. *MINING ENGINEERING*, *70*(6), 16. https://me.smenet.org/abstract.cfm?preview=1&articleID=8300&page=16

Pokhrel, N., Agioutanti, E., Keles, C., Afrouz, S., & Sarver, E. (2021). *Comparison of mineral content in respirable coal mine dust samples estimated using FTIR, TGA, and SEM-EDX*. 18th North American Mine Ventilation Symposium,

Sarver, E., Keles, C., & Rezaee, M. (2019). Beyond conventional metrics: Comprehensive characterization of respirable coal mine dust. *International Journal of Coal Geology*, *207*, 84-95. https://doi.org/10.1016/j.coal.2019.03.015

Soo, J.-C., Lee, T., Chisholm, W. P., Farcas, D., Schwegler-Berry, D., & Harper, M. (2016). Treated and untreated rock dust: Quartz content and physical characterization. *Journal of Occupational and Environmental Hygiene*, *13*(11), D201-D207. https://doi.org/10.1080/15459624.2016.1200195

Stach, R., Barone, T., Cauda, E., Krebs, P., Pejcic, B., Daboss, S., & Mizaikoff, B. (2020). Direct infrared spectroscopy for the size-independent identification and quantification of respirable particles relative mass in mine dusts. *Analytical and Bioanalytical Chemistry*, *412*(14), 3499-3508. https://doi.org/10.1007/s00216-020-02565-0

Chapter 3 – Summary of FTIR calibration data

Table 3-1 summarizes all the calibration factors available to estimate three mineral fractions (silica, kaolinite, and calcite) using the DOF FTIR method. The corresponding peak area for each mineral is divided by the provided factors to get a mass estimate of the mineral in the dust sample. 'Mine samples' refer to samples that are collected in the mine environment (in relatively low-concentration environments, and over longer sampling duration), and 'lab-generated samples' refer to samples that are collected in Virginia Tech laboratory in a sealed enclosure (in a relatively high-concentration environment, with short sampling duration). It is important to collect the calibration samples in a similar sampling environment and setup, that would be used to collect the samples for analysis.

Table 3-1 Summary of calibration factors for 3 different sampling conditions. All of the calibration factors are developed for coal mine samples collected in 37 mm polyvinyl chloride (PVC) filters using 10-mm nylon Dorr-Oliver cyclone. The corresponding peak area is divided by the given factors to get the mass estimate.

Analyte	Mine samples (2-piece)	Mine samples (3-piece)	Lab-generated samples (2-piece)
Silica (Q)	0.00465[a]	0.00530[d]	0.00695[e]
Kaolinite (K)	0.00227[b]	0.00259[a]	0.00339[c]
Calcite (Ca)	0.00223[c]	0.00255[c]	0.00334[e]

[a]Calculated using a 3-piece to 2-piece conversion factor (0.877) from Miller et al. (Miller et al., 2013).

[b]Calibration factor previously established by NIOSH using pure quartz/kaolinite calibration samples collected in 2-piece cassettes in a calm air dust chamber.

[c]Estimated using a ratio of calibration factors determined for RCS in sampling environments representative of the lab sampling conducted in the current study, and respirable coal mine dust sampling (as mentioned in Chapter 2, see Equation 2-2).

[d]Calibration factor extracted from the Field Analysis of Silica Tool (FAST) (NIOSH, 2019).

[e]Calculated in Virginia Tech laboratory in a sealed enclosure (see Figure 3-1).

Figure 3-1 shows the calibration curves for silica and calcite prepared using finely pulverized pure silica/calcite dust in a sealed enclosure in the Virginia Tech laboratory. The figures do not include the calibration curve for kaolinite because the factor calculated using the ratio described above in the footnotes of Table 3-1 (also mentioned in Chapter 2, Equation 2-2) was very similar to the one generated from the calibration curve for kaolinite.

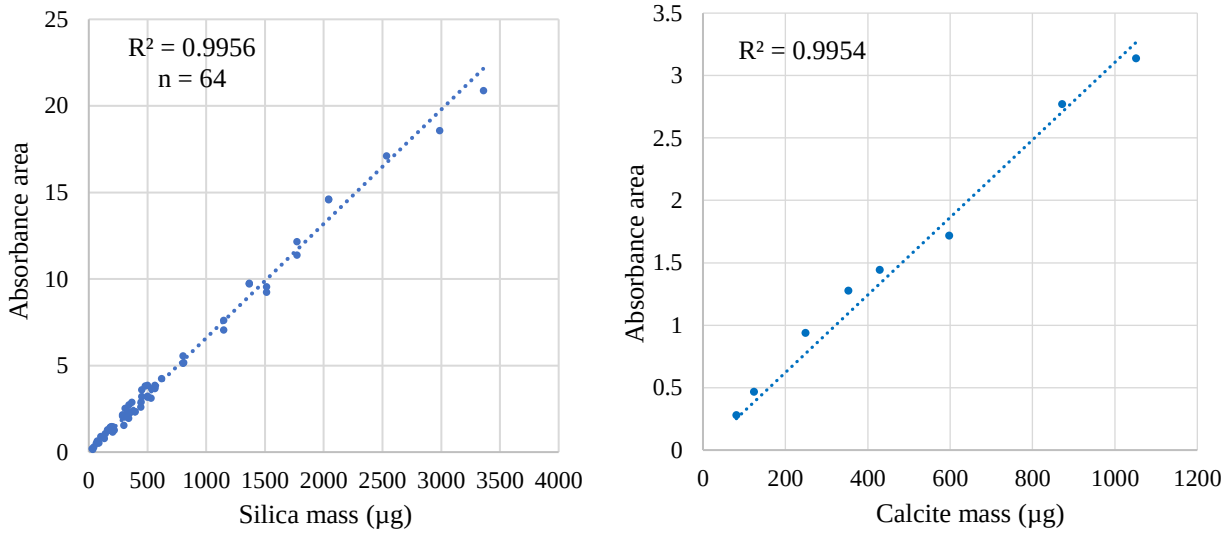

Figure 3-1. Calibration curves for (left) silica, and (right) calcite quantification model prepared using respirable samples of respirable pure silica or calcite. Y-axis shows the integrated absorbance peak area (between 890 to 865 cm^{-1} for calcite, and between 816 and 767 cm^{-1}) as a function of sample mass (µg) determined gravimetrically.

The limits of detection (LOD) and quantification (LOQ) based on integrated peak areas for silica, kaolinite, and calcite are summarized in Table 3-2 below. The LOD and LOQ for the FTIR instrument were estimated using the standard deviation of the corresponding peak area measurement of 20 blank PVC filters. LOD/LOQ for silica was derived from Cauda et al. (Cauda et al., 2016).

Table 3-2 Summary of LOD and LOQ of the portable FTIR instrument used in this study (based on integrated peak areas) for silica, kaolinite, and calcite.

Mineral	**LOD**	**LOQ**
Silica	0.026	0.078
Kaolinite	0.012	0.040
Calcite	0.003	0.010

REFERENCES

Cauda, E., Miller, A., & Drake, P. (2016). Promoting early exposure monitoring for respirable crystalline silica: Taking the laboratory to the mine site. *J Occup Environ Hyg*, *13*(3), D39-45. https://doi.org/10.1080/15459624.2015.1116691

Miller, A. L., Drake, P. L., Murphy, N. C., Cauda, E. G., LeBouf, R. F., & Markevicius, G. (2013). Deposition Uniformity of Coal Dust on Filters and Its Effect on the Accuracy of FTIR Analyses for Silica. *Aerosol Sci Technol*, *47*(7), 724-733. https://doi.org/10.1080/02786826.2013.787157

NIOSH. (2019). *FAST (Field Analysis of Silica Tool)*. In (Version Build 1.0.7.2) NIOSH-CDC. https://www.cdc.gov/niosh/mining/works/coversheet2056.html

Chapter 4 – Overall conclusions and recommendations for future work

This work contains two major efforts. Chapter 1 compared the mineral fraction (silica and kaolinite) estimated using the DOF FTIR method with mineral fractions from TGA and SEM-EDX. The results show the usefulness of the DOF FTIR method, especially for the estimation of kaolinite along with silica. Comparison of the methods suggested the presence of significant non-carbonate minerals other than silica and kaolinite in the coal mine dust. Results also show that the SEM-EDX frequently indicates much more mineral content—primarily other aluminosilicates—than that is predicted by either of the mass-based method: the FTIR and the TGA.

Chapter 2 dealt with exploring the DOF FTIR method to analyze additional minerals such as the calcite as a proxy for limestone rock dust in respirable dust samples collected in mines and also in the laboratory from major dust source materials (such as run-of-mine coal, rock strata, and rock dusting products). Results from 16 mines across the US show that calcite can serve as a suitable proxy for the rock dust contribution in respirable coal mine dust. Further, the DOF FTIR method also showed good agreement with TGA and SEM-EDX, and results were generally consistent with the expectation of dust contribution from sample source and mine sampling location.

Future work might deal with exploring possible interferences to calcite (or any other mineral) in the infrared spectra to refine the method. Additionally, calibration could be improved by using composite samples (containing several minerals, that sort of mimic the composition of real-world mine samples). The effect of particle size distribution on the calibration should also be further explored. Since the DOF FTIR method preserves the dust samples, further tests can be done on them. Therefore, to further develop the DOF FTIR method, the PVC samples could be analyzed by the standard MSHA P7 method, and the results could be compared. Additionally, the DOF FTIR method can also be used to further explore coal mine dust source apportionment, while also exploring other possible minerals (such as dolomite) that can be estimated using the infrared spectra.

Appendix A- Additional Tables and Figures

Table A-1. FTIR, TGA, and SEM-EDX results for respirable coal mine dust (RCMD) samples collected from 16 mines across the US.

No.	Mine		Loc	PVC Mass (mg)	FTIR (mass %)			TGA (mass %)			SEM-EDX (mass %)							
	Reg.	No.			Q	K	Ca	Coal	Carb	Non carb	C	MC	ASK	ASO	S	SLO	M	CB
1	SCA	10	B	0.148		24.7		25.4	3.7	70.9	17.8	16.6	25.7	32.7	5.6	0	0.8	0.8
2	SCA	10	B	0.181		26.4		26.8	5.5	67.7	3.8	8.9	47.1	35.3	3.7	0	0.3	1
3	SCA	10	F	0.132		23.6		41.7	3.5	54.8	11.3	7.9	32.3	35.3	8.3	0	3.9	0.9
4	SCA	10	F	0.183		18.3		43.6	16.8	39.6	8.3	7.7	37	44.2	1	0	2	0
5	SCA	10	I	0.005		na*	na*	84.4	1.8	13.7	22.6	14	5.4	9.1	41	1.3	0.4	6.2
6	SCA	10	P	0.089		29.9		na	na	na	na	na	na	na	na	na	na	na
7	SCA	10	P	1.494		21.3		22.7	3.2	74.1	0	0	83.5	15.8	0.7	0	0	0
8	SCA	10	R	0.038		38.1*	4.8*	62.3	3.3	34.4	28	13.2	23.8	24.9	8.3	0.2	0.3	1.3
9	SCA	11	B	0.106		24.4	6.3	36	9.3	54.7	1.2	5.2	11.8	60.4	14.2	0.2	1.2	5.8
10	SCA	11	F	0.164		14.2	3.9	54.4	6.9	38.7	23.5	10.8	11.2	30	11.1	0	7.8	5.6
11	SCA	11	P	1.153	6.2	11.9		11.4	4.9	83.7	0	0.1	3.8	95.4	0.8	0	0	0
12	SCA	11	R	0.749	6.7	13.9		25.8	5.2	69	0	0	1.8	97.5	0.7	0	0	0
13	SCA	12	B	0.103		21	22.5	55.1	13.4	31.4	32.1	16.5	9.7	19	4.2	1	1.4	16.1
14	SCA	12	I	0.054		35.3	18.4	76	5.4	18.6	56.7	8.2	7	11.7	5.3	0	0	11.1
15	SCA	12	P	1.077	4	12.8		29.5	4.8	65.6	7	7.5	29.6	52	3.4	0	0.4	0
16	SCA	12	R	0.649	3.2	15.3	1.9	20.8	7.4	71.7	0.1	0.6	7.2	91.3	0.7	0	0	0.1
17	SCA	13	B	2.535	12.3	10.1		13.6	5.8	80.6	0	0	2.1	96.8	1.1	0	0	0
18	SCA	13	F	0.189		8.4*	17.6	78	8.1	14	36.1	8.4	2.1	7.6	1.1	2.2	1.2	41.2
19	SCA	13	I	0.035		43.2*	87.2	39.9	26.8	33.3	6.5	1	1.3	5.7	1.4	0.1	0	84.1
20	SCA	13	I	0.701	4.6	5.9	9	62.9	12.8	24.4	23.1	10.5	3.7	41.3	7	0	0.3	14
21	SCA	13	R	1.297	1.8	2.6	4.6	73.9	4.4	21.7	58.9	10.8	5.4	15.4	4.1	0	0.1	5.4
22	SCA	13	R	7.347	4.7	1.5	69.7	8.1	69.5	22.4	0	0	0	9.5	0	5.4	0	85
23	SCA	14	B	0.039		42.8*	9.4*	29	12.5	58.6	10.5	6.9	27.9	32.2	16.6	0	2.6	3.2
24	SCA	14	F	0.187		19.1		27.5	5.1	67.4	2.3	4.5	10.6	53.3	13.2	2.1	1.4	12.7
25	SCA	14	I	0.002		na*	na*	66.7	9.2	24.1	8.6	3.8	4.3	16.8	8.7	0	0	57.9
26	SCA	14	P	4.348	7.3	11.3		9.5	4.7	85.8	0	0	2	97.9	0.1	0	0	0
27	MCA	15	B	0.145		19.6	16.5	30.3	10.8	58.9	14.9	8.4	11.4	24.2	22.7	0	5.5	12.9
28	MCA	15	F	0.028		56.4*	35.4	47.8	23.5	28.8	46.3	3.2	15	9.6	4.8	0	0	21.2
29	MCA	15	I	0.001		na*	na	73.8	-0.1	26.3	8.7	1.4	0	6.6	0	0	0.5	82.7
30	MCA	15	P	0.47	4.1	23.5	4.9	32.1	7.7	60.2	9.6	6.2	27.6	21.4	11.8	0	0	23.4
31	MCA	15	R	0.351	5.1	19.6	2.3	19.7	6.2	74	8	5.4	30.5	40.3	11.7	0	1.6	2.5
32	NA	16	B	0.089		21.1	14.3	72.1	5.4	22.5	51	7.4	10.4	4.7	4.6	0	5.2	16.7
33	NA	16	F	0.073		35.6	12.3	65	9	26.1	41.8	11.2	25.6	10.8	2.5	0	0.6	7.7
34	NA	16	P	0.221		13.3	6.4	68	7.1	24.9	27.4	22.4	9.9	14.4	9.4	1.6	7.7	7.1
35	NA	16	R	0.172		14.9	12.2	62.3	9.7	28	53.5	14	7	9.5	4.4	0	3.7	8
36	NA	17	B	0.043		39.3*	68.6	46.3	38.1	15.7	7.2	3	3.2	16.4	18	1.5	5.6	45
37	NA	17	I	0.016		90.5*	70.8	93.2	4.1	2.7	2.4	1.4	1.4	3.4	1.8	0	1.5	88.1
38	NA	17	I	0.072		36.5	14	61.6	6.3	32.1	24.7	5.3	32.9	19.8	4	0	0.3	13
39	NA	17	P	0.277		25.6	0.6*	34.9	4.8	60.3	2.5	5.3	42.2	47.1	0.9	0	0.4	1.6
40	NA	17	R	0.489		5.9	77.9	30.7	59	10.2	14.8	2.4	1.5	6.8	1	0.1	0.9	72.5
41	NA	17	R	0.763	1.9	21.5		35.4	3.4	61.3	0	0	59	40.3	0.7	0	0	0
42	NA	18	B	0.096		33.3	6.1	31.7	9.8	58.5	26.4	5.7	27.2	20.1	8.3	0.1	4.2	7.9
43	NA	18	F	0.018		na	27	71.3	6.4	22.3	24.1	5.4	16.2	17.4	4.3	0.5	1.4	30.7
44	NA	18	I	0.002		na*	na*	67.7	12.2	20.1	7.9	1.8	4	3.8	1.2	0	1.1	80
45	NA	18	P	0.34		21.9		39.5	5.7	54.9	1	1.4	38.2	54.5	2.8	0	0	2.1
46	NA	18	R	0.231		22.9	2.2	41.5	7.7	50.8	21.7	10.5	34.5	25.3	6.8	0.1	0	1.1
47	MW	19	B	0.181		15.1	7.3	56.9	9	34.1	8	21.3	1.4	48.7	7.7	0	0.7	12.2
48	MW	19	F	2.608	4.6	7.7	4.6	48.4	6.1	45.5	0.4	1.6	3.8	82.2	10.6	0.2	0.4	0.8
49	MW	19	I	0.014		76.0*	52.9	0	48.8	51.3	15.7	13.9	2.5	24.4	4.8	0.8	1.6	36.3
50	MW	19	P	0.277		8.3	22.3	49.5	16.7	33.8	13.6	11.6	0	32.4	3.5	0.2	5.8	32.8
51	MW	19	R	0.223		11.2	7.8	47.2	5	47.8	13.8	19.6	8	48.8	5.1	0.2	1.7	2.9
52	MW	19	R	0.299		7.4	24.9	45.2	20.6	34.2	9.8	19.9	0.1	37.8	4.2	0.5	2.8	25
53	MW	20	B	0.53		9.4	31	32	21.4	46.6	0	1.5	0.1	68.1	1	0	0.7	28.6

54	MW	20	F	0.143		13.3	37.5	32.1	35.9	32	27.3	6	1.6	16.6	7.8	0	2.4	38.4
55	MW	20	F	0.191		11.2	25.1	36.6	21.2	42.2	19.4	10.7	3.5	28.2	6	0.1	0.1	32.1
56	MW	20	I	0.019		54.9*	na	57.5	28.3	14.1	16.8	7.5	0.5	2.6	3.8	0.6	3.4	64.7
57	MW	20	P	0.758	0.5*	9	7.8	31.4	8.6	60	0	0	0.2	94.8	0.6	0	0	4.3
58	MW	20	R	0.577		9.7	9.7	32.7	11.1	56.2	7.7	19.6	2.9	45.4	2.8	0	1.3	20.2
59	SCA	21	B	0.085		20.5*	19.3	46.5	10.2	43.3	4.7	8.4	7.9	37.2	15.1	0.1	1.2	25.4
60	SCA	21	F	0.089		21	4.6*	15.8	2.8	81.5	6.3	10.1	15.9	47.9	11.8	0	3.3	4.6
61	SCA	21	I	0.063		27.6*	9	60.8	5.6	33.6	7.8	8.7	18.4	42.8	10.1	0	2	10.1
62	SCA	21	P	1.415	5.2	12		8.1	4.1	87.9	0	0	1.5	98.1	0.4	0	0	0
63	SCA	21	R	0.557	4.4	12.8		8.7	4.2	87.1	0	0	5.4	93.7	0.8	0	0	0
64	SCA	22	F	0.018		78.1*		61.9	5.2	33	40	10.6	3.9	9.7	6.3	0	26.5	3
65	SCA	22	I	0.003		na*		89.7	6.3	4.1	40.3	11.6	9.5	19.3	8.8	0	1.3	9.2
66	SCA	22	P	1.23	7	7.2		34.2	16.3	49.5	0	0	0.5	98.2	1.3	0	0	0
67	W	23	I	0.097		10.7*	37.2	30.6	58.7	10.6	6.3	1.3	0	2.2	0	0	0	90.3
68	W	23	I	0.176		8.3*	38.1	40.8	50.7	8.5	15.3	4.3	0	1.3	0.8	0.1	0.5	77.7
69	W	23	I	na	na	na*	na	67.8	18	14.3	65.9	3.9	1.5	1.2	4.2	0	5.8	17.5
70	W	23	P	0.268		4.1*	93.7	n/a	n/a	n/a	na	na	na	na	na	na	na	na
71	W	23	P	0.349		3.9*	100	5.8	68	26.2	1.4	0.9	0	0.2	0.1	0	0.1	97.3
72	W	23	R	0.888		4.1	72.3	29	62.1	8.9	1.3	1.8	0	0.6	0.1	0	0	96.2
73	W	24	F	0.068		22.8*	16.5	70.9	9.8	19.3	37	7.1	0.2	10.7	5.5	0.2	0.1	39.1
74	W	24	I	0.052		21.1*	23.9	68.2	15.9	15.9	27.8	7.8	2	10.1	4.7	1.2	0.3	46.1
75	W	24	I	0.063		24.1*	32.4	53	20	27	23.6	2.8	0	7.5	4	1.7	2.3	58.1
76	W	24	I	1.547	24.9	6.6	1.6	30.7	2.9	66.4	0.6	1.3	0	3	94.6	0.4	0	0
77	W	24	R	0.165		11.8	23.5	43.7	14	42.3	14.6	7.8	0.4	19.5	20.4	1.8	0	35.5
78	W	24	R	5.361	3.5	3.2	97.1	12.3	70.2	17.6	0.3	0.2	0	5.7	0	0.9	0	93
79	SCA	25	B	0.416	8.65	21.7		39	6.1	54.9	0	0.3	18	76.7	5	0	0	0
80	SCA	25	F	0.336	5.63	13		40.3	8.3	51.8	2.7	7.5	9.6	64.2	6.7	0.2	2.5	6.6
81	SCA	25	I	0.01			na*	77.4	0.7	21.8	7.2	9.1	17.3	43	8.6	1.1	1.2	12.5
82	SCA	25	P	0.088	2.62		4	42.7	8.3	49	6.3	8.8	33.7	28.3	9.1	0	2.2	11.7
83	SCA	25	P	0.189	4.65			18.4	7.2	74.4	6.9	11.1	32.6	31.5	12.2	0	5.5	0.1
84	SCA	25	P	0.227	3.1			29.1	1.1	69.8	2.9	6.3	35.9	42.3	7.7	0.1	2.4	2.3
85	SCA	25	P	0.311	5.48			26.9	9.8	63.3	1.9	7.5	23.4	50	4.8	0	0.8	11.7
86	SCA	25	P	0.357	4.24			57.3	6.1	36.6	0.5	3.9	15.7	71	5.3	0	0.7	3
87	SCA	25	P	0.596	7			13.8	5.1	81.1	0.1	0.1	26.5	71.1	0.7	0	0	1.5
88	SCA	25	P	0.669	5.59			42.3	1	56.7	0	0.7	37.4	59.5	2.1	0.1	0.2	0
89	SCA	25	P	0.949	7.29			13.9	7.6	78.5	0	0.1	28.6	69.7	1.6	0	0	0
90	SCA	25	R	0.069	8.14		3.2*	52.6	20	27.4	8.3	9.6	29.5	34.8	6.9	0.1	3	7.9
91	SCA	25	R	0.13	2.41		3.2*	22.1	6.2	71.6	11.5	12.6	24.1	24.9	13.7	0	0.8	12.4
92	SCA	25	R	0.132	4.43			23.3	6.1	70.6	7.3	8.6	27.9	42.4	6.6	0	3.8	3.5
93	SCA	25	R	0.202	3.03			18.3	6.3	75.4	11.3	9.1	27.3	32.2	12	0.2	5.4	2.5

*samples between LOD and LOQ
na*: data unavailable (these samples are between LOD and LOQ, and have very low/missing sample mass)
na: data unavailable
empty cells: samples below LOD, with negative peak area
Note: the sample numbers assigned in the first column is not consistent across tables 1-3 and Table A-1.

Table A-2. FTIR, TGA, and SEM-EDX results for respirable dust samples generated from mine dust source materials.

No.	Mine No.	Source Material	PVC Mass (mg)	†† FTIR (mass %)			§ TGA (mass %)			§ SEM-EDX (mass %)							
				Q	K	Ca	Coal	Carb.	Non carb.	C	MC	ASK	ASO	S	SLO	M	CB
1	10	BD	1.050	15.6	20.6	0‡	11.3	5.22	83.45	0.2	1.4	29.0	50.5	16.5	0.3	1.6	0.5
2	13	BD	1.025	34.5	11.4	0‡	9.6	6.04	84.34	1.5	5.9	21.5	36.4	24.1	1.8	8.3	0.4
3	14	BD	0.982	11.7	10.8	0‡	8.3	7.39	84.28	0.2	1.7	21.8	57.1	17.8	0.2	1.1	0.1
4	16	BD	1.088	42.1	31.2	0‡	5.6	7.54	86.87	0.4	1.3	21.6	33.6	41.1	1.7	0.3	0.0
5†	17	BD	0.716	26.3	28.2	0‡	6.5	10.39	83.12	3.0	4.3	34.3	22.8	34.5	0.1	0.0	0.9
6	18	BD	1.028	32.1	22.5	0‡	9.5	5.53	85.01	1.3	6.4	32.6	34.7	19.7	0.2	5.2	0.0
7	19	BD	1.053	9.9	3.4	61.6	6.2	60.77	32.98	1.7	2.4	0.0	10.6	5.9	3.5	0.0	75.9
8	20	BD	1.075	1.7	1.8	81.2	3.5	84.14	12.37	1.4	1.1	0.1	13.5	3.2	1.8	0.1	78.9
9	21	BD	1.007	26.1	15.3	0‡	10.0	6.58	83.45	1.2	2.5	27.7	57.2	8.8	0.1	2.2	0.4
10	22	BD	1.090	17.1	9.2	0‡	7.5	10.92	81.56	0.8	4.6	31.6	45.9	15.1	0.0	2.0	0.0

11	23	BD	1.005	24.5	25.5	0‡	26.6	4.46	68.98	13.9	11.4	10.6	42.8	15.0	0.2	5.0	1.1
12	24	BD	1.021	71.7	10.6	0‡	19.8	1.98	78.17	3.2	3.1	3.8	14.3	75.3	0.0	0.0	0.1
13	12	C	1.044	9.4	8.5	1.0	58.7	11.51	29.83	64.2	12.1	8.8	4.9	10.0	0.0	0.0	0.1
14†	13	C	1.020	1.9	0‡	3.0	78.3	21.68	0.00	92.3	3.4	0.0	0.0	2.0	0.0	0.0	2.3
15	14	C	0.915	0.5	1.1	0.5	90.1	5.31	4.58	80.7	7.0	5.6	3.0	3.7	0.0	0.0	0.0
16	15	C	1.057	3.0	3.5	0.5	68.5	31.53	0.00	65.5	5.9	12.4	3.1	8.3	0.0	4.8	0.0
17	16	C	1.213	3.8	11.5	7.6	67.1	12.90	20.04	29.3	9.6	30.5	10.7	6.1	0.6	1.0	12.2
18	17	C	0.885	0.2	3.8	0.9	86.3	8.06	5.63	84.3	2.6	6.1	2.5	1.6	0.0	0.9	2.0
19	18	C	1.068	2.6	9.0	0‡	74.8	8.12	17.12	49.0	9.0	29.0	6.9	4.3	0.0	1.1	0.8
20	19	C	0.897	1.0	5.1	0.8	79.4	4.07	16.56	51.7	12.2	9.9	2.1	10.3	0.3	6.2	7.3
21†	21	C	1.262	0.6	0‡	1.3	79.4	20.62	0.00	78.2	5.7	3.2	5.1	7.6	0.0	0.1	0.0
22†	22	C	0.859	2.9	4.4	0.4	75.4	14.13	10.49	40.7	8.6	22.3	20.9	6.7	0.0	0.2	0.6
23	23	C	0.907	0.4	6.9	0.9	77.3	2.41	20.33	67.2	10.1	8.7	6.5	4.5	0.0	0.0	2.9
24†	11	RD	1.271	0‡	0.7‡	91.0	1.1	92.75	6.19	1.0	0.1	0.0	0.1	0.0	0.0	0.0	98.8
25†	12	RD	1.065	0‡	1.4*	92.6	4.3	88.34	7.34	0.3	0.4	0.2	0.9	0.0	1.3	0.0	96.9
26†	13	RD	1.050	0.2‡	0‡	63.0	4.9	95.06	0.00	0.8	0.4	0.0	0.8	0.0	0.1	0.0	98.0
27†	14	RD	0.954	0‡	0.7‡	94.7	2.1	92.34	5.54	1.0	1.1	0.0	1.7	0.3	0.0	0.2	95.7
28†	15	RD	1.223	0.8‡	0.4‡	89.4	6.2	85.79	8.03	0.2	0.3	0.0	1.0	0.2	0.0	0.1	98.2
29†	16	RD	1.159	0‡	1.2*	88.7	0.0	96.23	3.77	0.4	0.3	0.1	1.4	0.3	0.0	0.0	97.6
30†	17	RD	1.238	0.6*	0.8‡	106.8	1.0	95.72	3.33	0.8	0.9	0.0	1.5	0.5	0.0	0.0	96.4
31†	18	RD	0.822	0‡	0.6‡	103.1	2.9	93.23	3.90	0.0	0.1	0.0	0.2	0.0	0.0	0.0	99.7
32†	19	RD	0.896	1.4*	1.9*	89.4	2.4	85.57	12.07	0.3	0.6	0.0	1.5	0.5	0.3	0.0	96.8
33†	20	RD	1.059	0.2‡	0.6‡	93.6	4.2	91.42	4.35	0.4	0.3	0.0	0.2	0.0	0.0	0.0	99.1
34†	22	RD	0.942	0‡	1*	93.7	0.6	93.84	5.51	0.2	0.1	0.0	0.1	0.1	0.0	0.0	99.6
35†	23	RD	0.844	0.1‡	0.6‡	95.1	3.9	93.80	2.27	0.6	0.4	0.0	0.3	0.1	0.0	0.3	98.3
36†	24	RD	0.933	0‡	1.4*	95.9	2.6	93.14	4.30	1.3	0.6	0.0	0.4	0.0	0.4	0.0	97.3
37	10	RR	1.077	11.7	25.1	0‡	32.7	6.50	60.75	3.7	3.4	46.1	36.7	8.3	0.0	0.2	1.7
38	11	RR	1.074	22.9	15.8	0‡	8.6	6.09	85.27	0.2	1.4	22.8	68.9	6.4	0.2	0.1	0.0
39	12	RR	1.028	15.1	17.5	0‡	8.0	6.72	85.24	1.7	5.5	18.6	53.6	15.2	0.2	4.9	0.4
40	14	RR	1.075	21.1	12.3	0‡	8.4	6.67	84.90	0.1	1.2	21.0	63.1	12.7	0.1	1.9	0.0
41	15	RR	1.009	16.6	15.6	0‡	17.9	10.01	72.06	3.3	3.4	38.5	36.9	17.3	0.0	0.6	0.0
42	18	RR	1.615	17.8	24.7	0‡	9.6	5.33	85.12	0.9	2.2	52.6	35.0	8.0	0.0	0.0	1.4
43	19	RR	1.091	13.0	8.4	4.0	21.4	7.05	71.55	4.0	11.7	3.0	43.2	35.1	0.6	0.0	2.3
44†	21	RR	0.820	19.5	14.0	0‡	6.5	6.14	87.35	0.7	2.3	33.8	50.2	10.9	0.1	1.9	0.2
45†	22	RR	0.851	12.9	10.0	0‡	10.7	7.69	81.59	2.8	2.0	38.9	40.3	14.4	0.2	1.3	0.1
46	23	RR	0.863	30.7	34.0	0‡	41.9	2.72	55.42	9.9	8.0	22.2	39.2	20.6	0.1	0.0	0.0

‡ FTIR samples below LOD.

* Samples between LOD and LOQ.

** The provided sample mass is the average of multiple (either 2 or 3) PVC samples collected for each material.

† Only 2 samples collected from this material was used to get the average sample mass and FTIR data. Rest are the average from 3 samples.

†† FTIR data is the average of either 2 or 3 replicate samples for each material.

§ All TGA and SEM-EDX data come from a single sample for each material.

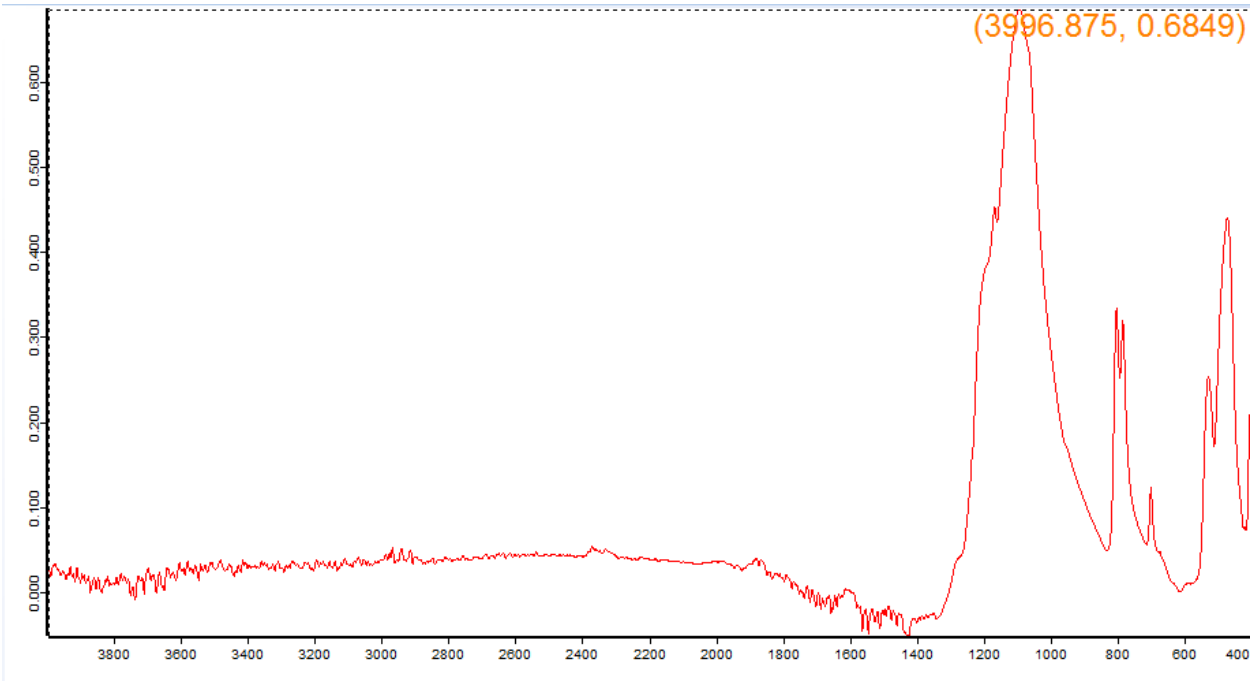

Figure A-1. Infrared spectra obtained from a pure silica (MIN-U-SIL 5) dust sample captured by the portable FTIR instrument, and processed using OPUS software (Version 8.2.28, 32 bit).

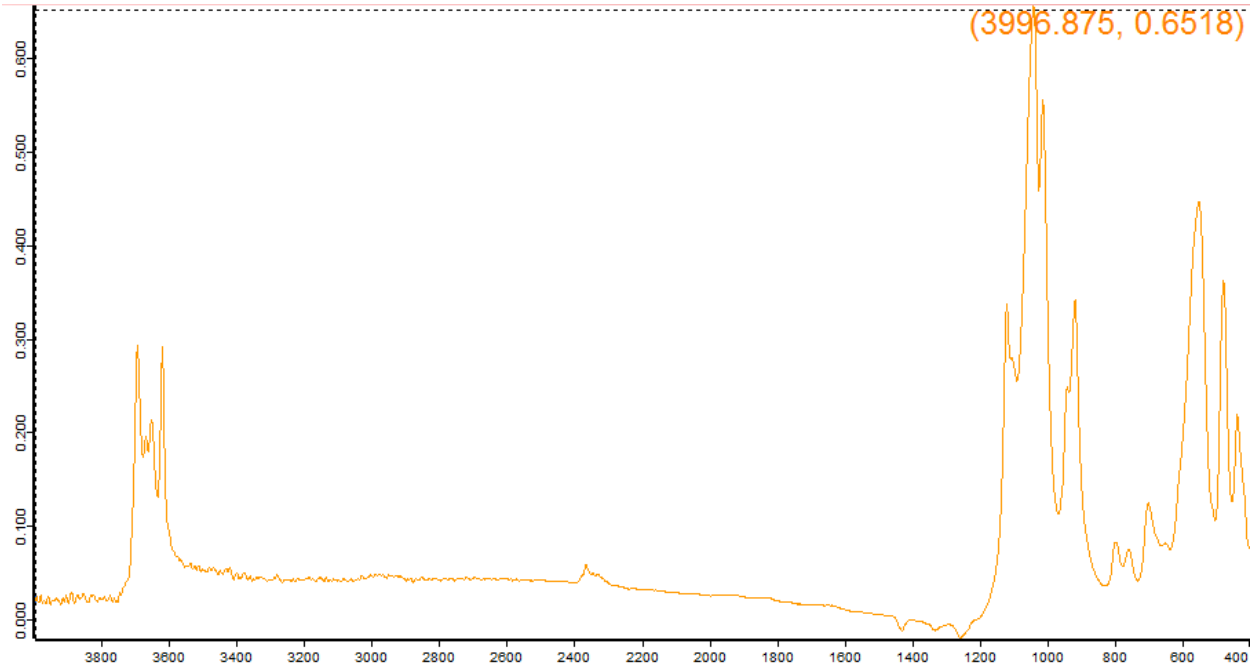

Figure A-2. Infrared spectra obtained from a pure kaolinite dust sample captured by the portable FTIR instrument, and processed using OPUS software (Version 8.2.28, 32 bit).

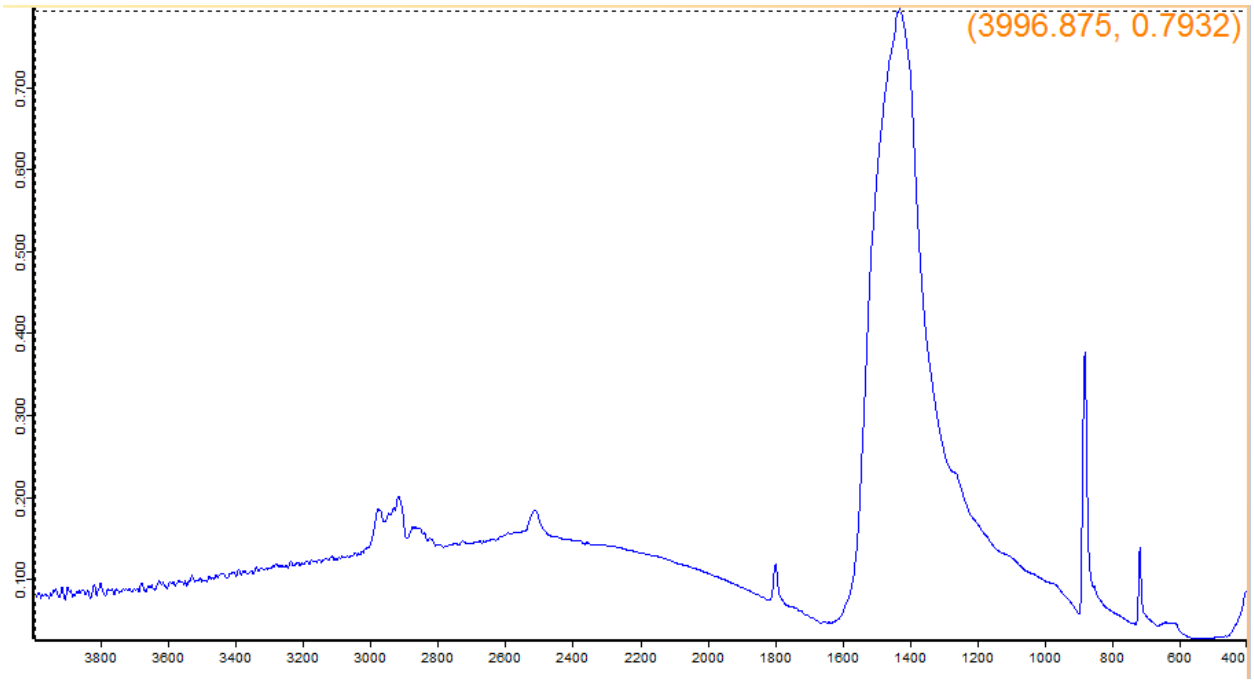

Figure A-3. Infrared spectra obtained from a pure calcium carbonate (calcite) dust sample captured by the portable FTIR instrument, and processed using OPUS software (Version 8.2.28, 32 bit).

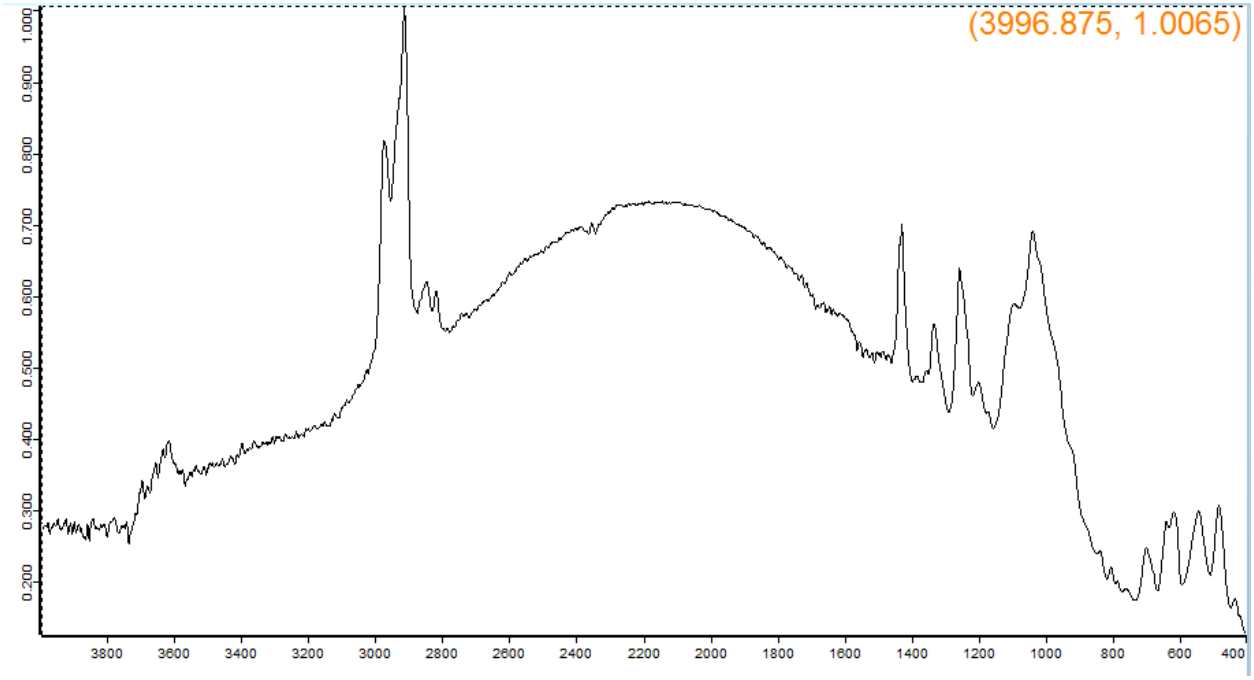

Figure A-4. Infrared spectra obtained from a respirable coal mine dust (RCMD) sample captured by the portable FTIR instrument, and processed using OPUS software (Version 8.2.28, 32 bit).